The Astrophysical Journal, 795:142 (23pp), 2014 November 10 doi:10.1088/0004-637X/795/2/142

DEFINING PHOTOMETRIC PECULIAR TYPE Ia SUPERNOVAE

S. González-Gaitán[1,2], E. Y. Hsiao[3], G. Pignata[1,4], F. Förster[1,5], C. P. Gutiérrez[1,2], F. Bufano[1,4], L. Galbany[1,2], G. Folatelli[6], M. M. Phillips[3], M. Hamuy[1,2], J. P. Anderson[7], and T. de Jaeger[1,2]
[1] Millennium Institute of Astrophysics, Casilla 36-D, Santiago, Chile; sgonzale@das.uchile.cl
[2] Departamento de Astronomía, Universidad de Chile, Camino El Observatorio 1515, Las Condes, Santiago, Chile
[3] Carnegie Observatories, Las Campanas Observatory, Casilla 601, La Serena, Chile
[4] Departamento de Ciencias Físicas, Universidad Andres Bello, Avda. Republica 252, Santiago, Chile
[5] Centro de Modelamiento Matemático, Universidad de Chile, Av. Blanco Encalada 2120 Piso 7, Santiago, Chile
[6] Kavli Institute for the Physics and Mathematics of the Universe, the University of Tokyo, Kashiwa 277-8583 (Kavli IPMU, WPI), Japan
[7] European Southern Observatory, Alonso de Córdova 3107, Casilla 19, Santiago, Chile
Received 2014 June 26; accepted 2014 September 16; published 2014 October 23

ABSTRACT

We present a new photometric identification technique for SN 1991bg-like type Ia supernovae (SNe Ia), i.e., objects with light curve characteristics such as later primary maxima and the absence of a secondary peak in redder filters. This method is capable of selecting this sub-group from the normal type Ia population. Furthermore, we find that recently identified peculiar sub-types such as SNe Iax and super-Chandrasekhar SNe Ia have photometric characteristics similar to 91bg-like SNe Ia, namely, the absence of secondary maxima and shoulders at longer wavelengths, and can also be classified with our technique. The similarity of these different SN Ia sub-groups perhaps suggests common physical conditions. This typing methodology permits the photometric identification of peculiar SNe Ia in large upcoming wide-field surveys either to study them further or to obtain a pure sample of normal SNe Ia for cosmological studies.

Key words: cosmology: miscellaneous – supernovae: general

Online-only material: color figures

1. INTRODUCTION

Despite great progress over recent years from the observational as well as from the theoretical perspective, the nature of type Ia supernovae (SNe Ia) remains elusive and under active debate. These luminous explosions have been used to obtain cosmological parameters with increasing precision (Riess et al. 1998; Perlmutter et al. 1999; Conley et al. 2011; Suzuki et al. 2012), yet the progenitor system still remains unknown. A key to unveiling their origin relies in the study and understanding of the intrinsic diversity seen in their light curves and colors, whose cosmic evolution also ultimately affects cosmology through systematics.

In fact, SNe Ia constitute a heterogeneous sample with differing light curves whose primary variety is well explained by the relations of luminosity and light curve shape (Phillips 1993), and of luminosity and color (Riess et al. 1996; Tripp 1998). The variation of light curve shape and luminosity is attributed to the amount of ^{56}Ni produced in thermonuclear runaway of the exploding carbon–oxygen white dwarf (CO-WD; Mazzali et al. 2007). The nature of the companion star of the binary system and the physics of the explosion are still unknown. Models include single-degenerate scenarios with a non-degenerate companion and the WD exploding near the Chandrasekhar mass (e.g., Nomoto et al. 1984; Hachisu et al. 1996; Dessart et al. 2014) or at sub-Chandrasekhar mass (Nomoto 1982; Sim et al. 2010; Kromer et al. 2010), as well as double-degenerate scenarios with two WDs slowly coalescing (Lorén-Aguilar et al. 2009; Shen et al. 2012) or merging in a violent fashion (Iben & Tutukov 1984; Pakmor et al. 2012; Kromer et al. 2013b), and even more exotic channels (Kashi & Soker 2011; Wheeler 2012). See Maoz et al. (2014) for a review.

Extreme cases and outliers in the SN Ia population were recognized early on: overluminous SNe Ia or SN 1991T-like objects (e.g., Filippenko et al. 1992b; Phillips et al. 1992; Maza et al. 1994), and subluminous or SN 1991bg-like ones (e.g., Filippenko et al. 1992a; Leibundgut et al. 1993; Hamuy et al. 1994). These objects make up a considerable fraction of SNe Ia (Li et al. 2011; Smartt et al. 2009, ∼40%) and represent a key ingredient for understanding the SN Ia mechanism. Furthermore, in recent years, new interesting outliers have further challenged the general SN Ia picture adding more heterogeneity and complexity: peculiar 2002cx-like SNe or "SNe Iax" (e.g., Li et al. 2003; Foley et al. 2013), super-Chandrasekhar-mass candidates (e.g., Howell et al. 2006; Scalzo et al. 2012), and some peculiar SNe with few representatives in their groups: SN 2000cx-like (Li et al. 2001; Candia et al. 2003; Silverman et al. 2013b), SN 2006bt (Foley et al. 2010b), and PTF 10ops-like with 91bg-like SN Ia characteristics, yet with wide light curve (Maguire et al. 2011; Kromer et al. 2013b). Also, there is recent evidence for SNe Ia with possible circumstellar material (CSM) interaction (Hamuy 2003; Dilday et al. 2012; Silverman et al. 2013a). Finally, new intriguing objects borderline of thermonuclear explosions are emerging: the calcium-rich SN group (Ca-rich: Perets et al. 2010, 2011b; Valenti et al. 2014a; Kasliwal et al. 2012) and extremely underluminous "SN.Ia" candidates (Kasliwal et al. 2010 although see Drout et al. 2013, 2014).

This plethora of thermonuclear events asks for an urgent classification scheme and hopefully a proper theoretical explanation of the diversity of observables that will link them together to possible progenitor channels. The investigation of the characteristics of all these objects can help us carve the way. The method presented in this paper is such an attempt based solely on photometry and light curve analysis of a large public SN Ia data set.

The original aim of the present work was to separate SN 1991bg SNe Ia from the normal population in an efficient, purely photometric fashion. Several studies of 91bg-like SNe Ia have been undertaken in the past (Garnavich et al. 2004; Taubenberger et al. 2008; Kasliwal et al. 2008). These SNe are known to

Table 1
Final Cuts and Errors Based on the Bootstrap Analysis with the Respective Number of Objects of Each Group Passing Each Cut

Cut	Normal SNe Ia	Peculiar SNe Ia[a]	91BG-like SNe Ia	SNe Iax	Super-CH SNe Ia[b]	CC SNe
None	602	59	35	13	5	321
SiFTO fit and LC coverage and $\Delta\chi^2_\nu > 0$	322	48	29	10	4	64
χ^2_ν(Ia) $< (34.0 \pm 6.65)$ χ^2_ν(91bg) $< (21.69 \pm 4.00)$[c]	304	45	29	8	4	43
Color–color relation $(u-B)_{10} > (0.18 \pm 0.13)$ $(B-V)_{10} < 0.7(u-B)_{10} + (0.77 \pm 0.23)$	299	44	29	7	2	17
$\Delta\chi^2_{\nu,\mathrm{blue}} > (-0.77 \pm 2.21)$ $\Delta\chi^2_{\nu,\mathrm{red}} > (2.83 \pm 3.11)$	263	31	19	6	2	5
Efficiency	81.7 ± 0.9	$64.6^{+2.1}_{-8.4}$	$65.5^{+0.0}_{-0.0}$	$60.0^{+10.0}_{-10.0}$	$50.0^{+25.0}_{-0.0}$	...
Purity	99.6 ± 0.0	$88.6^{+9.8}_{-3.6}$	$86.4^{+15.9}_{-3.9}$	$85.7^{+12.5}_{-33.7}$	$100.0^{+0.0}_{-32.2}$	...
FoM	81.4 ± 0.9	$57.2^{+0.0}_{-7.6}$	$56.6^{+10.4}_{-2.6}$	$51.4^{+9.8}_{-23.6}$	$50.0^{+25.0}_{-32.2}$	...

Notes. Final efficiencies, purities, and FoMs for some of our samples are presented.
[a] Peculiar SNe Ia include 91bg-like, SNe Iax, super-Ch, 00cx-like, and Ca-rich SNe Ia.
[b] Super-Ch candidates by Scalzo et al. (2012) are not included.
[c] This cut is applied to objects with better overall 91bg template fits and it requires enough data coverage in blue and red bands. Objects passing it are 91bg-like candidates and the others are other peculiar SNe Ia.

be fainter with mag$(B) \gtrsim -18$ at maximum and to have a faster light curve decline than their normal counterparts. Such a behavior has been best portrayed by light curve parameters such as Δm_{15} and stretch from different fitters (e.g., Hamuy et al. 1996b; Riess et al. 1996; Jha et al. 2007; Perlmutter et al. 1997; Guy et al. 2007), always putting 91bg-like SNe Ia at the faint and fast extreme of the light curve width–luminosity relation with $\lesssim$0.75 or $\Delta m_{15}(B) \gtrsim 1.7$. In addition, 91bg-like events are much cooler, as seen through their spectra with the presence of strong Ti II lines and their red colors, $(B-V)_{B_{\max}} \gtrsim 0.3$. Such a deviation from the normal population has made them unsuitable for cosmology. The different color evolution is particularly striking in the redder optical bands and the near-infrared (NIR) where neither shoulder nor secondary maxima are observed as opposed to classical SNe Ia (Phillips 2012). The color evolution also presents other less noticeable differences in the relative time of maximum light in the different bands: 91bg-like SNe Ia have maxima in the redder bands that occur after the maximum in bluer bands, whereas for normal events it happens before. These different features can been explained with the differing spectroscopic and color evolution of SNe Ia (e.g., Kasen & Woosley 2007): 91bg-like objects are cooler, therefore redder, and the recombination temperature of Fe III to Fe II for them occurs earlier. The onset of this recombination determines the red and NIR secondary maxima since the Fe II line blanketing absorbs flux in the blue that is re-emitted at longer wavelengths.

The 91bg-like photometric typing technique we present here reveals surprising adequacy to adjust other peculiar SNe Ia that have atypical light curves, such as SNe Iax, SN 2006bt-like, and super-Chandrasekhar SNe Ia, and the possibility of photometrically classifying them as well. In the current and coming age of large, wide-field surveys such as the Dark Energy Survey (DES; Sako et al. 2011a) and the Large Synoptic Survey Telecope (LSST; Ivezic et al. 2011), where thousands of transients are routinely discovered and the spectroscopic follow-up becomes expensive, the need of a photometric identification technique that provides a way of classifying and recognizing different sub-groups of SNe Ia for different scientific studies becomes imperative.

The paper is organized as follows. In Section 2, we present the data, as well as our photometric typing technique based on light curve fits, validating it with different light curve and spectroscopic diagnostics. Section 3 presents the results of the classification for different sub-samples of SNe Ia, and in Section 4, we investigate contamination from core-collapse (CC) SNe, the relevance and impact of the training sample used in the classification, and finally we look for possible common physical origins of the similar photometric SN Ia groups. We summarize in Section 5.

2. ANALYSIS

2.1. Data

In this work, we make use of several large, low-redshift ($z < 0.1$) SN Ia samples from the literature. Multi-band photometry is available for more than 500 SNe Ia obtained through the effort of several teams, including the Calán/Tololo survey (Hamuy et al. 1996a), the Carnegie Supernova Project CSP (Contreras et al. 2010; Stritzinger et al. 2011), the Center for Astrophysics CfA (Hicken et al. 2009, 2012), the Lick Observatory Supernova Search (Ganeshalingam et al. 2010), and many more. Besides analyzing SN photometry obtained exclusively after 1980, initially we do not have any restrictions on the source of the photometry used; as long as it is internally consistent, we do not require the type of precise calibration needed for cosmology. In order to test the typing technique, we also use a collection of nearby CC SNe from the literature. A summary of the number of SNe before and after the different light curve cuts we will apply is shown in Table 1. A list of SNe Ia used and their sources is presented in Table 2 and of CC SNe in Table 3.

2.2. Methodology: Light Curve Fits

We use here SiFTO (Conley et al. 2008) to fit the optical light curves of all SNe Ia with two different templates that reproduce the aforementioned differences between normal and 91bg-like SNe Ia. SiFTO is a powerful and versatile light curve fitter that manipulates spectral templates to simultaneously match the multi-band photometric data of a particular SN with heliocentric redshift z_{hel}. The spectral template at a given epoch t is adjusted to the observer frame fluxes through multiplicative factors n_f. A stretch parameterization s is used to describe the shape of the light curve and is defined as a factor multiplying the time axis (Perlmutter et al. 1997; Goldhaber et al. 2001). The time of peak luminosity in B, t_0, is an additional fit parameter. The light curve fit thus minimizes following χ^2 function:

$$\chi^2 = \sum_{j=1}^{N_f} \sum_{i=1}^{N_j} \frac{\left[F_j(t, t_0, n_f, s, z_{\mathrm{hel}}) - f_{ij}\right]^2}{\sigma_{ij}^2}, \qquad (1)$$

Table 2
Nearby SNe Ia Used in This Study Requiring Enough Light Curve Coverage

Name	Type	χ^2_ν(Ia)	χ^2_ν(91bg)	Source
PTF09dav	SN Ia-Ca	8.20	3.86	Sullivan et al. (2011)
PTF10bjs	SN Ia	5.86	20.13	Hicken et al. (2012)
PTF10ops	SN Ia	9.99	2.08	Maguire et al. (2011)
SN 1980N	SN Ia	5.19	8.16	Hamuy et al. (1991)
SN 1981B	SN Ia	15.24	26.41	Barbon et al. (1982)
SN 1981D	SN Ia	0.84	1.28	Hamuy et al. (1991)
SN 1982W	SN Ia	574.22	437.40	Barbon et al. (1989)
SN 1983G	SN Ia	32.59	36.41	Younger & van den Bergh (1985); Benetti et al. (1991); Cadonau & Leibundgut (1990)
SN 1983R	SN Ia	6.76	28.75	Barbon et al. (1989)
SN 1984A	SN Ia	40.34	47.68	Barbon et al. (1989); Cadonau & Leibundgut (1990)
SN 1986G	SN Ia	3.17	3.84	Phillips et al. (1987)
SN 1987N	SN Ia	165.36	72.33	Benetti et al. (1991)
SN 1989A	SN Ia	15.05	39.19	Tsvetkov et al. (1990); Benetti et al. (1991)
SN 1989B	SN Ia	0.76	5.41	Wells et al. (1994)
SN 1989M	SN Ia	75.69	54.19	Kimeridze & Tsvetkov (1991)
SN 1990af	SN Ia	1.02	8.04	Hamuy et al. (1996a)
SN 1990N	SN Ia	3.72	111.73	Lira et al. (1998)
SN 1991T	SN Ia	16.18	56.79	Altavilla et al. (2004); Ford et al. (1993); Lira et al. (1998)
SN 1992A	SN Ia	4.77	49.99	Altavilla et al. (2004)
SN 1992al	SN Ia	0.52	13.91	Hamuy et al. (1996a)
SN 1992bc	SN Ia	3.60	28.25	Hamuy et al. (1996a)
SN 1992bh	SN Ia	0.68	11.32	Hamuy et al. (1996a)
SN 1992bo	SN Ia	1.49	28.63	Hamuy et al. (1996a)
SN 1992bp	SN Ia	2.23	14.75	Hamuy et al. (1996a)
SN 1993ag	SN Ia	1.20	13.21	Hamuy et al. (1996a)
SN 1993H	SN Ia	1.59	5.77	Altavilla et al. (2004); Hamuy et al. (1996a)
SN 1993O	SN Ia	1.99	15.01	Hamuy et al. (1996a)
SN 1994ae	SN Ia	1.85	27.15	Altavilla et al. (2004); Riess et al. (2005)
SN 1994D	SN Ia	13.32	82.56	Altavilla et al. (2004); Meikle et al. (1996); Patat et al. (1996)
SN 1994S	SN Ia	2.72	22.02	Riess et al. (1999)
SN 1995ac	SN Ia	5.78	16.08	Riess et al. (1999)
SN 1995al	SN Ia	0.48	10.81	Riess et al. (1999)
SN 1995bd	SN Ia	4.00	39.46	Altavilla et al. (2004); Riess et al. (1999)
SN 1995D	SN Ia	1.44	21.59	Riess et al. (1999); Sadakane et al. (1996)
SN 1995E	SN Ia	0.89	11.77	Riess et al. (1999)
SN 1996bl	SN Ia	2.13	27.31	Riess et al. (1999)
SN 1996bo	SN Ia	10.30	78.58	Riess et al. (1999)
SN 1996X	SN Ia	1.44	26.53	Riess et al. (1999); Salvo et al. (2001)
SN 1997bp	SN Ia	12.78	30.81	Jha et al. (2006)
SN 1997bq	SN Ia	18.57	58.35	Jha et al. (2006)
SN 1997br	SN Ia	26.09	29.77	Jha et al. (2006)
SN 1997cy	SN Ia	396.02	433.18	Germany et al. (2000)
SN 1997do	SN Ia	6.17	58.89	Jha et al. (2006)
SN 1997E	SN Ia	3.55	41.39	Jha et al. (2006)
SN 1998ab	SN Ia	15.68	30.14	Jha et al. (2006)
SN 1998aq	SN Ia	2.25	40.51	Riess et al. (2005)
SN 1998bp	SN Ia	12.78	9.88	Jha et al. (2006)
SN 1998bu	SN Ia	2.84	55.73	Suntzeff et al. (1999)
SN 1998dh	SN Ia	4.19	46.18	Ganeshalingam et al. (2010); Jha et al. (2006)
SN 1998dm	SN Ia	2.98	77.41	Ganeshalingam et al. (2010); Jha et al. (2006)
SN 1998ef	SN Ia	8.81	27.35	Ganeshalingam et al. (2010); Jha et al. (2006)
SN 1998es	SN Ia	1.33	22.18	Jha et al. (2006)

Table 2
(Continued)

Name	Type	χ^2_ν(Ia)	χ^2_ν(91bg)	Source
SN 1999aa	SN Ia	2.08	50.11	Altavilla et al. (2004); Jha et al. (2006)
SN 1999ac	SN Ia	9.07	15.53	Jha et al. (2006); Phillips et al. (2006)
SN 1999ar	SN Ia	2.99	7.30	Kowalski et al. (2008)
SN 1999aw	SN Ia	5.61	45.58	Strolger et al. (2002)
SN 1999bi	SN Ia	1.94	3.47	Kowalski et al. (2008)
SN 1999bm	SN Ia	1.86	3.02	Kowalski et al. (2008)
SN 1999bn	SN Ia	1.18	2.08	Kowalski et al. (2008)
SN 1999bp	SN Ia	3.35	15.11	Kowalski et al. (2008)
SN 1999by	SN Ia	84.91	4.51	Ganeshalingam et al. (2010); Garnavich et al. (2004)
SN 1999cc	SN Ia	2.01	17.25	Jha et al. (2006); Krisciunas et al. (2006)
SN 1999cl	SN Ia	8.50	35.70	Ganeshalingam et al. (2010); Jha et al. (2006); Krisciunas et al. (2006)
SN 1999cp	SN Ia	12.71	106.37	Ganeshalingam et al. (2010); Krisciunas et al. (2000)
SN 1999da	SN Ia	51.58	5.05	Krisciunas et al. (2001)
SN 1999dg	SN Ia	3.78	17.68	Ganeshalingam et al. (2010)
SN 1999dk	SN Ia	3.45	29.17	Altavilla et al. (2004); Ganeshalingam et al. (2010); Krisciunas et al. (2001)
SN 1999dq	SN Ia	2.64	25.98	Jha et al. (2006)
SN 1999ee	SN Ia	2.97	87.85	Stritzinger et al. (2002)
SN 1999ej	SN Ia	1.83	21.49	Ganeshalingam et al. (2010)
SN 1999ek	SN Ia	2.35	43.79	Jha et al. (2006); Krisciunas et al. (2004b)
SN 1999gp	SN Ia	5.50	38.02	Ganeshalingam et al. (2010); Jha et al. (2006); Krisciunas et al. (2001)
SN 2000cn	SN Ia	5.25	22.19	Ganeshalingam et al. (2010); Jha et al. (2006)
SN 2000cu	SN Ia	1.66	14.02	Ganeshalingam et al. (2010)
SN 2000cw	SN Ia	2.32	11.04	Ganeshalingam et al. (2010)
SN 2000cx	SN Ia	12.55	47.15	Altavilla et al. (2004); Candia et al. (2003); Jha et al. (2006)
SN 2000dk	SN Ia	8.40	38.14	Ganeshalingam et al. (2010); Jha et al. (2006)
SN 2000dm	SN Ia	2.03	33.25	Ganeshalingam et al. (2010)
SN 2000dn	SN Ia	1.43	14.89	Ganeshalingam et al. (2010)
SN 2000dr	SN Ia	5.59	8.08	Ganeshalingam et al. (2010)
SN 2000E	SN Ia	5.88	36.99	Lair et al. (2006); Tsvetkov (2006a); Valentini et al. (2003)
SN 2000fa	SN Ia	2.90	33.51	Ganeshalingam et al. (2010); Jha et al. (2006)
SN 2001ah	SN Ia	0.77	2.55	Ganeshalingam et al. (2010); Hicken et al. (2009)
SN 2001ba	SN Ia	2.12	29.69	Krisciunas et al. (2004a)
SN 2001bf	SN Ia	18.83	28.94	Hicken et al. (2009)
SN 2001bt	SN Ia	2.78	28.56	Krisciunas et al. (2004b)
SN 2001cj	SN Ia	1.51	24.88	Ganeshalingam et al. (2010)
SN 2001ck	SN Ia	0.90	9.59	Ganeshalingam et al. (2010)
SN 2001cp	SN Ia	2.31	33.93	Ganeshalingam et al. (2010); Hicken et al. (2009)
SN 2001cz	SN Ia	1.79	56.26	Krisciunas et al. (2004b)
SN 2001da	SN Ia	6.73	30.56	Hicken et al. (2009)
SN 2001dl	SN Ia	2.58	32.75	Ganeshalingam et al. (2010)
SN 2001E	SN Ia	2.13	12.39	Ganeshalingam et al. (2010)
SN 2001eh	SN Ia	1.55	24.29	Hicken et al. (2009)
SN 2001el	SN Ia	6.06	44.16	Krisciunas et al. (2003)
SN 2001en	SN Ia	3.06	90.01	Hicken et al. (2009)
SN 2001ep	SN Ia	7.37	35.13	Hicken et al. (2009)
SN 2001ex	SN Ia	7.77	2.94	Ganeshalingam et al. (2010)
SN 2001fe	SN Ia	0.63	12.62	Hicken et al. (2009)

Table 2
(Continued)

Name	Type	χ^2_ν(Ia)	χ^2_ν(91bg)	Source
SN 2001fh	SN Ia	36.94	68.47	Hicken et al. (2009)
SN 2001V	SN Ia	1.50	30.45	Hicken et al. (2009)
SN 2002bf	SN Ia	1.85	8.61	Hicken et al. (2009); Leonard et al. (2005)
SN 2002bo	SN Ia	4.67	44.03	Benetti et al. (2004); Ganeshalingam et al. (2010); Hicken et al. (2009)
SN 2002cd	SN Ia	6.38	47.28	Hicken et al. (2009)
SN 2002cf	SN Ia	10.07	3.40	Ganeshalingam et al. (2010)
SN 2002cr	SN Ia	4.49	61.34	Hicken et al. (2009)
SN 2002cs	SN Ia	30.25	21.43	Ganeshalingam et al. (2010)
SN 2002cu	SN Ia	3.90	50.32	Ganeshalingam et al. (2010)
SN 2002cv	SN Ia	6.48	11.68	Elias-Rosa et al. (2008)
SN 2002cx	SN Iax	18.30	10.79	Phillips et al. (2007)
SN 2002de	SN Ia	3.89	33.39	Hicken et al. (2009)
SN 2002dj	SN Ia	5.03	60.16	Ganeshalingam et al. (2010); Hicken et al. (2009); Pignata et al. (2008)
SN 2002dl	SN Ia	18.48	20.28	Ganeshalingam et al. (2010)
SN 2002dp	SN Ia	4.70	54.32	Hicken et al. (2009)
SN 2002eb	SN Ia	2.72	39.65	Ganeshalingam et al. (2010)
SN 2002ef	SN Ia	3.66	29.35	Ganeshalingam et al. (2010)
SN 2002el	SN Ia	2.69	46.33	Ganeshalingam et al. (2010)
SN 2002er	SN Ia	3.39	48.05	Ganeshalingam et al. (2010); Pignata et al. (2004)
SN 2002es	SN Ia	27.61	7.09	Ganeshalingam et al. (2012); Hicken et al. (2009)
SN 2002fb	SN Ia	32.41	2.14	Hicken et al. (2009)
SN 2002fk	SN Ia	3.69	60.81	Hicken et al. (2009)
SN 2002ha	SN Ia	4.33	60.43	Hicken et al. (2009)
SN 2002he	SN Ia	4.00	59.38	Hicken et al. (2009)
SN 2002hu	SN Ia	2.29	26.25	Hicken et al. (2009)
SN 2002hw	SN Ia	4.68	35.88	Hicken et al. (2009)
SN 2002jg	SN Ia	3.16	39.55	Ganeshalingam et al. (2010)
SN 2003ae	SN Ia	28.64	11.89	Hicken et al. (2009)
SN 2003cg	SN Ia	4.04	43.52	Elias-Rosa et al. (2006); Ganeshalingam et al. (2010); Hicken et al. (2009)
SN 2003du	SN Ia	5.09	55.52	Anupama et al. (2005); Hicken et al. (2009); Leonard et al. (2005)
SN 2003fa	SN Ia	2.15	39.49	Hicken et al. (2009)
SN 2003gn	SN Ia	1.84	14.44	Ganeshalingam et al. (2010)
SN 2003gq	SN Ia	26.99	4.46	Ganeshalingam et al. (2010)
SN 2003gt	SN Ia	4.68	90.25	Ganeshalingam et al. (2010)
SN 2003fg	SN Ia-supCh	11.54	4.60	Howell et al. (2006)
SN 2003he	SN Ia	2.65	29.34	Ganeshalingam et al. (2010)
SN 2003it	SN Ia	0.75	6.60	Hicken et al. (2009)
SN 2003iv	SN Ia	0.59	17.95	Hicken et al. (2009)

Table 2
(Continued)

Name	Type	χ^2_ν(Ia)	χ^2_ν(91bg)	Source
SN 2003kc	SN Ia	5.20	10.39	Hicken et al. (2009)
SN 2003kf	SN Ia	4.26	35.76	Hicken et al. (2009)
SN 2003U	SN Ia	2.44	35.24	Hicken et al. (2009)
SN 2003W	SN Ia	8.21	41.90	Hicken et al. (2009)
SN 2003Y	SN Ia	21.85	3.04	Ganeshalingam et al. (2010)
SN 2004as	SN Ia	2.07	16.48	Hicken et al. (2009)
SN 2004br	SN Ia	5.33	58.42	Ganeshalingam et al. (2010)
SN 2004bv	SN Ia	3.85	49.51	Ganeshalingam et al. (2010)
SN 2004bw	SN Ia	2.14	32.02	Ganeshalingam et al. (2010)
SN 2004ef	SN Ia	4.71	69.01	Contreras et al. (2010)
SN 2004eo	SN Ia	7.64	43.43	Contreras et al. (2010)
SN 2004ey	SN Ia	2.62	86.19	Contreras et al. (2010)
SN 2004fu	SN Ia	2.48	22.22	Hicken et al. (2009); Tsvetkov (2006b)
SN 2004fz	SN Ia	9.80	87.89	Ganeshalingam et al. (2010)
SN 2004gs	SN Ia	3.43	16.71	Contreras et al. (2010)
SN 2004gu	SN Ia	2.44	48.96	Contreras et al. (2010)
SN 2005A	SN Ia	23.31	59.97	Contreras et al. (2010)
SN 2005ag	SN Ia	1.12	17.09	Contreras et al. (2010)
SN 2005al	SN Ia	1.57	36.33	Contreras et al. (2010)
SN 2005am	SN Ia	2.54	35.40	Contreras et al. (2010)
SN 2005bc	SN Ia	3.13	26.53	Ganeshalingam et al. (2010)
SN 2005bl	SN Ia	29.66	3.50	Contreras et al. (2010)
SN 2005cf	SN Ia	4.06	41.67	Hicken et al. (2009); Pastorello et al. (2007); Wang et al. (2009b)
SN 2005de	SN Ia	5.07	75.35	Ganeshalingam et al. (2010)
SN 2005dm	SN Ia	21.16	2.55	Ganeshalingam et al. (2010)
SN 2005el	SN Ia	2.52	28.56	Contreras et al. (2010)
SN 2005eq	SN Ia	1.37	32.54	Contreras et al. (2010)
SN 2005eu	SN Ia	5.93	37.69	Hicken et al. (2009)
SN 2005gj	SN Ia	247.03	151.35	Prieto et al. (2007)
SN 2005hc	SN Ia	1.08	20.40	Contreras et al. (2010)
SN 2005hj	SN Ia	4.60	25.15	Stritzinger et al. (2011); Hicken et al. (2009)
SN 2005hk	SN Iax	100.24	17.06	Hicken et al. (2009); McCully et al. (2014); Phillips et al. (2007)
SN 2005iq	SN Ia	4.18	75.47	Stritzinger et al. (2011); Hicken et al. (2009)
SN 2005ir	SN Ia	2.75	17.46	Stritzinger et al. (2011)
SN 2005kc	SN Ia	5.09	75.65	Stritzinger et al. (2011); Hicken et al. (2009)
SN 2005ke	SN Ia	79.61	4.41	Stritzinger et al. (2011); Hicken et al. (2009)
SN 2005ki	SN Ia	1.80	37.62	Stritzinger et al. (2011); Hicken et al. (2009)
SN 2005lz	SN Ia	2.51	6.76	Hicken et al. (2009)
SN 2005M	SN Ia	2.07	50.93	Stritzinger et al. (2011)
SN 2005ms	SN Ia	3.50	38.91	Hicken et al. (2009)
SN 2005mz	SN Ia	22.50	5.98	Hicken et al. (2009)
SN 2005na	SN Ia	2.38	53.92	Stritzinger et al. (2011); Hicken et al. (2009)
SN 2005W	SN Ia	5.39	78.59	Stritzinger et al. (2011)
SN 2006ac	SN Ia	2.27	27.59	Hicken et al. (2009)
SN 2006ar	SN Ia	5.88	41.52	Hicken et al. (2009)
SN 2006ax	SN Ia	2.40	74.01	Stritzinger et al. (2011); Hicken et al. (2009)
SN 2006az	SN Ia	3.50	24.36	Hicken et al. (2009)
SN 2006bh	SN Ia	1.88	60.14	Stritzinger et al. (2011)
SN 2006bt	SN Ia	6.94	8.06	Stritzinger et al. (2011); Hicken et al. (2009)
SN 2006bz	SN Ia	15.10	3.31	Hicken et al. (2009)
SN 2006cc	SN Ia	3.73	36.85	Hicken et al. (2009)
SN 2006cp	SN Ia	2.36	24.62	Hicken et al. (2009)
SN 2006cq	SN Ia	2.14	8.60	Hicken et al. (2009)

Table 2
(Continued)

Name	Type	χ^2_ν(Ia)	χ^2_ν(91bg)	Source
SN 2006D	SN Ia	3.13	41.76	Stritzinger et al. (2011)
SN 2006dd	SN Ia	6.73	55.36	Stritzinger et al. (2011)
SN 2006dm	SN Ia	2.01	30.52	Ganeshalingam et al. (2010)
SN 2006ef	SN Ia	3.32	66.58	Stritzinger et al. (2011); Hicken et al. (2009)
SN 2006ej	SN Ia	2.53	36.34	Stritzinger et al. (2011); Hicken et al. (2009)
SN 2006em	SN Ia	11.72	2.31	Hicken et al. (2009)
SN 2006et	SN Ia	2.37	51.53	Stritzinger et al. (2011); Hicken et al. (2009)
SN 2006eu	SN Ia	6.34	2.14	Hicken et al. (2009)
SN 2006fw	SN Ia	24.11	29.39	Stritzinger et al. (2011)
SN 2006gj	SN Ia	3.41	12.94	Stritzinger et al. (2011); Hicken et al. (2009)
SN 2006gr	SN Ia	3.04	19.81	Hicken et al. (2009)
SN 2006gt	SN Ia	2.59	5.05	Stritzinger et al. (2011)
SN 2006gz	SN Ia-supCh	26.04	21.65	Hicken et al. (2007)
SN 2006ha	SN Ia	2.50	1.65	Hicken et al. (2009)
SN 2006hx	SN Ia	8.34	39.02	Stritzinger et al. (2011)
SN 2006ke	SN Ia	43.28	3.00	Hicken et al. (2009)
SN 2006kf	SN Ia	2.69	45.59	Stritzinger et al. (2011); Hicken et al. (2009)
SN 2006le	SN Ia	2.32	36.66	Hicken et al. (2009)
SN 2006lf	SN Ia	2.45	44.13	Hicken et al. (2009)
SN 2006mo	SN Ia	4.36	16.27	Hicken et al. (2009)
SN 2006mp	SN Ia	1.28	15.39	Hicken et al. (2009)
SN 2006mr	SN Ia	84.22	9.38	Stritzinger et al. (2011)
SN 2006nz	SN Ia	6.80	4.15	Hicken et al. (2009)
SN 2006oa	SN Ia	1.78	9.06	Hicken et al. (2009)
SN 2006ob	SN Ia	1.82	11.25	Stritzinger et al. (2011); Hicken et al. (2009)
SN 2006qo	SN Ia	1.71	33.12	Hicken et al. (2009)
SN 2006S	SN Ia	3.04	25.87	Hicken et al. (2009)
SN 2006sr	SN Ia	2.06	27.67	Hicken et al. (2009)
SN 2006X	SN Ia	6.84	53.81	Stritzinger et al. (2011)
SN 2007af	SN Ia	1.36	38.75	Stritzinger et al. (2011); Hicken et al. (2009)
SN 2007au	SN Ia	18.30	22.29	Hicken et al. (2009)
SN 2007ax	SN Ia	62.76	5.45	Stritzinger et al. (2011); Hicken et al. (2009)
SN 2007ba	SN Ia	10.98	8.63	Stritzinger et al. (2011); Hicken et al. (2009)
SN 2007bc	SN Ia	1.93	32.47	Stritzinger et al. (2011); Hicken et al. (2009)
SN 2007bd	SN Ia	4.87	85.43	Stritzinger et al. (2011); Hicken et al. (2009)
SN 2007bm	SN Ia	2.50	80.15	Stritzinger et al. (2011); Hicken et al. (2009)
SN 2007ca	SN Ia	4.11	56.21	Stritzinger et al. (2011); Hicken et al. (2009)
SN 2007ci	SN Ia	37.97	38.69	Hicken et al. (2009)
SN 2007co	SN Ia	2.80	49.56	Hicken et al. (2009)

Table 2
(Continued)

Name	Type	χ^2_ν(Ia)	χ^2_ν(91bg)	Source
SN 2007cp	SN Ia	14.98	37.09	Hicken et al. (2009)
SN 2007cq	SN Ia	1.62	24.66	Hicken et al. (2009)
SN 2007cv	SN Ia	0.73	8.08	Brown et al. (2009)
SN 2007F	SN Ia	1.90	55.47	Hicken et al. (2009)
SN 2007fr	SN Ia	3.74	4.32	Ganeshalingam et al. (2010)
SN 2007gi	SN Ia	3.58	10.71	Zhang et al. (2010)
SN 2007hj	SN Ia	7.73	8.24	Ganeshalingam et al. (2010); Hicken et al. (2012)
SN 2007jg	SN Ia	1.59	12.72	Stritzinger et al. (2011); Hicken et al. (2012)
SN 2007jh	SN Ia	24.92	14.55	Stritzinger et al. (2011)
SN 2007kd	SN Ia	56.18	8.38	Hicken et al. (2012)
SN 2007ke	SN Ia-Ca	1.12	1.12	Kasliwal et al. (2012)
SN 2007kk	SN Ia	1.75	7.01	Hicken et al. (2012)
SN 2007le	SN Ia	5.57	70.85	Stritzinger et al. (2011); Hicken et al. (2012)
SN 2007mm	SN Ia	15.99	3.92	Stritzinger et al. (2011)
SN 2007N	SN Ia	82.36	7.29	Stritzinger et al. (2011); Hicken et al. (2009)
SN 2007nq	SN Ia	1.89	31.24	Stritzinger et al. (2011); Hicken et al. (2012)
SN 2007on	SN Ia	25.54	25.37	Stritzinger et al. (2011)
SN 2007qd	SN Iax	5.76	2.83	McClelland et al. (2010)
SN 2007qe	SN Ia	5.06	47.56	Hicken et al. (2009)
SN 2007R	SN Ia	4.19	23.67	Hicken et al. (2009)
SN 2007S	SN Ia	1.87	48.23	Stritzinger et al. (2011); Hicken et al. (2009)
SN 2007sw	SN Ia	3.21	16.14	Hicken et al. (2012)
SN 2007ux	SN Ia	3.92	4.94	Ganeshalingam et al. (2010); Hicken et al. (2012)
SN 2008A	SN Iax	33.73	18.87	Ganeshalingam et al. (2010); Hicken et al. (2012)
SN 2008ae	SN Iax	97.41	21.83	Foley et al. (2013); Hicken et al. (2012)
SN 2008ar	SN Ia	1.07	10.38	Ganeshalingam et al. (2010); Hicken et al. (2012)
SN 2008bc	SN Ia	6.63	134.01	Stritzinger et al. (2011)
SN 2008bf	SN Ia	2.62	37.87	Hicken et al. (2009)
SN 2008cm	SN Ia	1.57	28.12	Hicken et al. (2012)
SN 2008dr	SN Ia	3.45	18.23	Ganeshalingam et al. (2010); Hicken et al. (2012)
SN 2008ec	SN Ia	2.71	39.71	Ganeshalingam et al. (2010)
SN 2008fp	SN Ia	1.81	68.68	Stritzinger et al. (2011)
SN 2008fv	SN Ia	13.91	34.08	Biscardi et al. (2012); Tsvetkov & Elenin (2010)
SN 2008ge	SN Iax	8.84	3.83	Foley et al. (2010a)
SN 2008gl	SN Ia	1.03	16.41	Hicken et al. (2012)
SN 2008gp	SN Ia	2.55	107.52	Stritzinger et al. (2011)
SN 2008gy	SN Ia	2.41	12.75	Tsvetkov et al. (2010)
SN 2008ha	SN Iax	14.36	4.29	Stritzinger et al. (2014); Valenti et al. (2009)
SN 2008hm	SN Ia	2.44	13.57	Hicken et al. (2012)
SN 2008hs	SN Ia	5.93	26.03	Hicken et al. (2012)
SN 2008hv	SN Ia	2.47	51.50	Stritzinger et al. (2011); Hicken et al. (2012)
SN 2008ia	SN Ia	5.04	66.72	Stritzinger et al. (2011)
SN 2008J	SN Ia	81.20	35.50	Taddia et al. (2012a)
SN 2008L	SN Ia	2.55	42.55	Ganeshalingam et al. (2010); Hicken et al. (2009)
SN 2008R	SN Ia	12.02	32.41	Stritzinger et al. (2011)
SN 2008Z	SN Ia	5.80	46.70	Ganeshalingam et al. (2010); Hicken et al. (2012)
SN 2009ad	SN Ia	0.88	12.53	Hicken et al. (2012)
SN 2009al	SN Ia	10.63	17.28	Hicken et al. (2012)
SN 2009an	SN Ia	2.42	46.74	Hicken et al. (2012)
SN 2009bv	SN Ia	2.77	20.21	Hicken et al. (2012)

Table 2
(Continued)

Name	Type	χ^2_ν(Ia)	χ^2_ν(91bg)	Source
SN 2009dc	SN Ia-supCh	30.09	13.00	Hicken et al. (2012); Stritzinger et al. (2011); Taubenberger et al. (2011)
SN 2009ds	SN Ia	6.15	56.25	Hicken et al. (2012)
SN 2009F	SN Ia	65.52	4.34	Stritzinger et al. (2011)
SN 2009gf	SN Ia	3.56	16.64	Hicken et al. (2012)
SN 2009ig	SN Ia	2.50	25.13	Foley et al. (2012); Hicken et al. (2012)
SN 2009kq	SN Ia	1.45	21.28	Hicken et al. (2012)
SN 2009le	SN Ia	1.49	95.55	Hicken et al. (2012)
SN 2009li	SN Ia	5.43	1.60	Hicken et al. (2012)
SN 2009na	SN Ia	1.40	22.70	Hicken et al. (2012)
SN 2009nr	SN Ia	3.88	5.44	Khan et al. (2011); Tsvetkov et al. (2011)
SN 2009Y	SN Ia	2.49	32.96	Hicken et al. (2012)
SN 2010A	SN Ia	0.75	17.12	Hicken et al. (2012)
SN 2010ae	SN Iax	61.63	11.32	Stritzinger et al. (2014)
SN 2010ai	SN Ia	2.07	42.80	Hicken et al. (2012)
SN 2010dt	SN Ia	1.13	6.77	Hicken et al. (2012)
SN 2010ev	SN Ia	4.86	38.75	C. P. Gutierrez et al. (2014, in preparation)
SN 2010Y	SN Ia	8.00	34.57	Hicken et al. (2012)
SN 2011aa	SN Ia	3.45	4.74	Brown et al. (2012)
SN 2011ay	SN Iax	2.14	0.76	Foley et al. (2013)
SN 2011fe	SN Ia	1.81	36.47	Richmond & Smith (2012)
SN 2012cg	SN Ia	10.27	98.30	Munari et al. (2013)
SN 2012dn	SN Ia	20.37	18.73	Brown et al. (2012); Chakradhari et al. (2014)
SN 2012Z	SN Iax	220.14	33.64	Foley et al. (2013)
SN 2013bh	SN Ia	5.24	3.94	Silverman et al. (2013b)
SN 2014J	SN Ia	7.74	66.38	Foley et al. (2014); Marion et al. (2014b); Tsvetkov et al. (2014)
LSQ12gdj	SN Ia-91T	5.86	94.77	Scalzo et al. (2014)
SNF20080514002	SN Ia	0.45	6.79	Brown et al. (2012)
SNF200705280	SN Ia-supCh	3.56	11.45	Scalzo et al. (2012)
SNF200708030	SN Ia-supCh	2.38	17.99	Scalzo et al. (2012)
SNF200709120	SN Ia-supCh	8.28	18.26	Scalzo et al. (2012)
SNF200805220	SN Ia-supCh	1.63	15.90	Hicken et al. (2012); Scalzo et al. (2012)
SNF200807230	SN Ia-supCh	6.24	12.03	Scalzo et al. (2012)

Notes. Reduced quality of fit (χ^2_ν) to normal and 91bg templates are shown.

where N_j is the number of data points in the jth filter for N_f filters, f_{ij} are the observed fluxes with corresponding errors σ_{ij}, and F_j is the modeled flux given by the integration of the spectral energy distribution (SED) through the given filter j at a certain epoch t and is dependent on the model parameters. The χ^2 is a general score of the fit taking all input bands together. The SiFTO color, $\mathcal{C}$, is obtained adjusting the SED to observed colors (via the normalization factors n_i) corrected only for Milky Way extinction with values from Schlafly & Finkbeiner (2011). No correction for the host reddening is attempted due to our poor understanding of it.

Given its nature, SiFTO is highly dependent on the spectral template series. We use the one developed by Hsiao et al. (2007) for normal SNe Ia, commonly used for cosmology (Conley et al. 2011) and other SN Ia studies (e.g., Pan et al. 2014), and the one

Table 3
Nearby CC SNe Used in This Study Requiring Enough Light Curve Coverage

Name	Type	χ^2_ν(Ia)	χ^2_ν(91bg)	Source
SN 1986I	SN II	14.70	12.72	Pennypacker et al. (1989)
SN 1987A	SN II	252.44	282.08	Hamuy et al. (1990); Bouchet et al. (1989)
SN 1988A	SN II	3.35	2.40	Benetti et al. (1991); Turatto et al. (1993)
SN 1988H	SN II	0.15	0.15	Turatto et al. (1993)
SN 1990E	SN II	41.89	20.40	Benetti et al. (1994); Schmidt et al. (1993)
SN 1990K	SN II	23.81	23.31	Cappellaro et al. (1995)
SN 1991G	SN II	100.56	126.02	Blanton et al. (1995)
SN 1992am	SN II	145.46	126.15	Schmidt et al. (1994)
SN 1994N	SN II	77.52	50.25	Pastorello et al. (2004)
SN 1994W	SN II	0.31	0.52	Sollerman et al. (1998)
SN 1995ad	SN II	34.30	26.92	Inserra et al. (2013a)
SN 1996W	SN II	48.16	10.06	Inserra et al. (2013a)
SN 1997D	SN II	44.03	55.90	Benetti et al. (2001)
SN 1999br	SN II	600.13	554.44	Pastorello et al. (2004)
SN 1999em	SN II	391.08	298.72	Hamuy et al. (2001); Leonard et al. (2002a)
SN 1999eu	SN II	25.75	45.89	Pastorello et al. (2004)
SN 1999gi	SN II	226.68	175.88	Leonard et al. (2002b)
SN 2000cb	SN II-pec	472.57	390.51	Kleiser et al. (2011)
SN 2001dc	SN II	38.82	35.56	Pastorello et al. (2004)
SN 2001X	SN II	48.41	41.99	Tsvetkov (2006a)
SN 2002bj	Peculiar SN	118.47	78.62	Poznanski et al. (2010)
SN 2002hh	SN II	38.96	33.61	Pozzo et al. (2006); Tsvetkov et al. (2007)
SN 2003hn	SN II	125.57	117.94	Krisciunas et al. (2009)
SN 2004A	SN II	315.26	198.97	Hendry et al. (2006); Tsvetkov (2008)
SN 2004dj	SN II	56.11	44.76	Chugai et al. (2005); Tsvetkov et al. (2008)
SN 2004ek	SN II	235.97	217.80	Tsvetkov (2008)
SN 2004et	SN II	362.17	362.66	Misra et al. (2007)
SN 2005ay	SN II	40.75	27.03	Tsvetkov et al. (2006)
SN 2005cs	SN II	418.69	341.36	Brown et al. (2007); Dessart et al. (2008); Pastorello et al. (2009)
SN 2006au	SN II	311.52	377.20	Taddia et al. (2012b)
SN 2006bc	SN II	598.27	517.52	Pritchard et al. (2014)
SN 2006bp	SN II	7.71	6.94	Dessart et al. (2008); Pritchard et al. (2014)
SN 2006V	SN II	585.76	688.07	Taddia et al. (2012b)
SN 2007aa	SN II	622.20	443.87	Pritchard et al. (2014)
SN 2007ck	SN II	1.45	1.94	Pritchard et al. (2014)
SN 2008aw	SN II	38.31	40.06	Pritchard et al. (2014)
SN 2008gz	SN II	64.48	26.55	Roy et al. (2011b)
SN 2008ij	SN II	12.01	7.88	Pritchard et al. (2014)
SN 2008in	SN II	295.20	296.59	Pritchard et al. (2014); Roy et al. (2011a)
SN 2008jb	SN II	4.95	5.06	Prieto et al. (2012)
SN 2008M	SN II	201.38	200.07	Pritchard et al. (2014)
SN 2009bw	SN II	114.11	88.44	Inserra et al. (2012)
SN 2009js	SN II	53.17	43.42	Gandhi et al. (2013)
SN 2009md	SN II	52.55	48.79	Fraser et al. (2011)
SN 2009N	SN II	541.98	481.67	Takáts et al. (2014)
SN 2010aq	SN II	70.17	71.52	Gezari et al. (2010)
SN 2010F	SN II	19.13	13.64	Pritchard et al. (2014)
SN 2010gs	SN II	2.87	2.98	Pritchard et al. (2014)
SN 2010id	SN II	57.11	44.72	Gal-Yam et al. (2011)
SN 2010kd	SN II	6.45	9.82	Pritchard et al. (2014)
SN 2011cj	SN II	3.94	4.39	Pritchard et al. (2014)
SN 2012A	SN II	115.75	93.09	Pritchard et al. (2014); Tomasella et al. (2013)
SN 2012ak	SN II	6.59	6.98	Pritchard et al. (2014)

Table 3
(Continued)

Name	Type	χ^2_ν(Ia)	χ^2_ν(91bg)	Source
SN 2012aw	SN II	381.27	265.25	Bose et al. (2013); Pritchard et al. (2014)
SN 2013ej	SN II	64.70	22.33	Valenti et al. (2014b)
CSS121015	SLSN	38.23	46.42	Benetti et al. (2014)
iPTF13bvn	SN Ib	50.12	15.48	Cao et al. (2013)
PS1–10bzj	SLSN-I	2.67	9.74	Lunnan et al. (2013)
PS1–11af	TDE?	15.56	10.33	Chornock et al. (2014)
PTF12dam	SLSN-Ic	383.86	240.18	Nicholl et al. (2013)
SN 1994I	SN Ic	62.15	6.81	Richmond et al. (1995)
SN 1994Y	SN IIn	196.97	109.15	Ho et al. (2001)
SN 1998bw	SN Ic	15.84	6.46	Clocchiatti et al. (2011); Galama et al. (1998); McKenzie & Schaefer (1999)
SN 1999el	SN IIn	27.52	22.72	Di Carlo et al. (2002)
SN 2002ap	SN Ic	44.87	16.76	Foley et al. (2003); Gal-Yam et al. (2002); Yoshii et al. (2003)
SN 2003jd	SN Ic	14.36	2.04	Valenti et al. (2008)
SN 2003lw	SN Ic	694.10	785.27	Malesani et al. (2004)
SN 2004aw	SN Ic	13.60	3.27	Taubenberger et al. (2006)
SN 2005bf	SN Ib	190.57	138.43	Folatelli et al. (2006)
SN 2005fk	SN Ic	1.09	1.08	Sako et al. (2014)
SN 2005hl	SN Ib	51.00	12.81	Sako et al. (2014)
SN 2005hm	SN Ib	20.24	9.58	Sako et al. (2014)
SN 2005kd	SN IIn	48.95	68.66	Pritchard et al. (2014)
SN 2005kj	IIn	370.95	296.60	Taddia et al. (2013)
SN 2005kr	SN Ic	4.22	1.70	Sako et al. (2014)
SN 2005ks	SN Ic	3.53	1.91	Sako et al. (2014)
SN 2005la	SN Ib/IIn	7.79	14.65	Pastorello et al. (2008)
SN 2005mn	SN IIP	123.07	70.69	D'Andrea et al. (2010)
SN 2006aa	IIn	924.91	731.05	Taddia et al. (2013)
SN 2006aj	SN Ic	10.09	3.60	Pian et al. (2006); Pritchard et al. (2014)
SN 2006bo	IIn	141.12	131.55	Taddia et al. (2013)
SN 2006fe	SN Ic	6.55	5.44	Sako et al. (2014)
SN 2006fo	SN Ib	67.96	23.99	Sako et al. (2014)
SN 2006gy	SN IIn	26.04	48.19	Agnoletto et al. (2009); Kawabata et al. (2009)
SN 2006jd	SN IIn	816.49	641.89	Pritchard et al. (2014); Stritzinger et al. (2012)
SN 2006jo	SN Ib	5.18	1.36	Sako et al. (2014)
SN 2006lc	SN Ic	63.56	14.35	Sako et al. (2014)
SN 2006nx	SN Ic	3.90	1.65	Sako et al. (2014)
SN 2006qk	SN Ib	1.05	1.06	Sako et al. (2014)
SN 2006qq	IIn	318.98	278.03	Taddia et al. (2013)
SN 2007bi	SN Ic-PI?	24.83	23.53	Gal-Yam et al. (2009); Young et al. (2010)
SN 2007gl	SN Ib	10.54	10.52	Sako et al. (2014)
SN 2007gr	SN Ic	33.34	16.20	Hunter et al. (2009)
SN 2007ms	SN Ic	12.55	3.12	Sako et al. (2014)
SN 2007nc	SN Ib	1.88	1.31	Sako et al. (2014)
SN 2007pk	SN IIn-P	31.96	11.45	Inserra et al. (2013a); Pritchard et al. (2014)
SN 2007qv	SN Ic	12.63	13.89	Sako et al. (2014)
SN 2007qw	SN Ib	4.98	2.10	Sako et al. (2014)
SN 2007qx	SN Ic	13.34	11.64	Sako et al. (2014)
SN 2007rt	SN IIn	350.31	320.86	Trundle et al. (2009)
SN 2007uy	SN Ib	23.01	4.77	Pritchard et al. (2014); Roy et al. (2013)
SN 2007Y	SN Ib	105.53	31.99	Pritchard et al. (2014); Stritzinger et al. (2009)
SN 2008aq	SN IIb	1.24	1.69	Pritchard et al. (2014)
SN 2008bo	SN Ib	41.23	30.58	Pritchard et al. (2014)

Table 3
(Continued)

Name	Type	χ^2_ν(Ia)	χ^2_ν(91bg)	Source
SN 2008D	SN Ib	53.29	18.94	Modjaz et al. (2009); Tanaka et al. (2009)
SN 2008fq	SN IIn	66.41	45.04	Taddia et al. (2013)
SN 2008iy	SN IIn	205.13	220.09	Miller et al. (2010)
SN 2008S	SN IIn-impost	20.47	18.55	Botticella et al. (2009); Smith et al. (2009)
SN 2009bb	SN Ic-BL	16.00	2.12	Pignata et al. (2011)
SN 2009ip	IIn-pec?	28.98	30.30	Fraser et al. (2013)
SN 2009jf	SN Ib	45.32	14.88	Pritchard et al. (2014); Sahu et al. (2011); Valenti et al. (2011)
SN 2009kn	SN IIn-P	62.39	60.30	Kankare et al. (2012)
SN 2009mg	SN IIb	3.73	3.40	Pritchard et al. (2014)
SN 2010ah	SN Ic	5.07	2.78	Corsi et al. (2011); Pritchard et al. (2014)
SN 2010bh	SN Ic	2.83	1.79	Bufano et al. (2012)
SN 2010bt	SN IIn	3.55	5.94	Pritchard et al. (2014)
SN 2010gx	SN Ic?ultra-b	15.53	43.39	Pastorello et al. (2010)
SN 2010jl	SN IIn	418.33	394.05	Pritchard et al. (2014); Stoll et al. (2011); Zhang et al. (2012)
SN 2010mc	SN IIn	14.70	7.93	Ofek et al. (2013)
SN 2010md	SLSN-Ic	15.52	4.57	Inserra et al. (2013b)
SN 2010O	Ib	42.83	5.48	Kankare et al. (2014)
SN 2010P	Ib	6.54	0.47	Kankare et al. (2014)
SN 2011am	SN Ib	8.04	5.49	Pritchard et al. (2014)
SN 2011bm	SN Ic	22.62	12.30	Valenti et al. (2012)
SN 2011dh	SN IIb	23.12	11.12	Marion et al. (2014a); Pritchard et al. (2014); Sahu et al. (2013)
SN 2011fu	SN IIb	62.50	30.23	Kumar et al. (2013)
SN 2011ht	SN IIn-P	32.98	30.63	Mauerhan et al. (2013); Pritchard et al. (2014)
SN 2011hw	SN IIn/Ibn	5.47	3.19	Pritchard et al. (2014); Smith et al. (2012)
SDSS4012	SN Ic	27.48	11.55	Sako et al. (2014)
SDSS14475	SN Ic	3.01	2.46	Sako et al. (2014)

Notes. Reduced quality of fit (χ^2_ν) to normal and 91bg-like SN Ia templates are shown.

Table 4
Comparison of Normal SN Ia Photometric Classification for Some of the Best Selected Published Techniques in Percentages

Technique	Efficiency (%)	Purity (%)	FoM (%)
Poznanski et al. (2007)	97	77–91	75–88
Rodney & Tonry (2009)	94	98	92
Sako et al. (2011b)	88–92	87–94	82–86
Olmstead et al. (2014)	85–92	89–93	79–83
This work	82	99	81

by Nugent et al. (2002)[8] for 91bg-like SNe Ia, previously used to identify objects with 91bg-like characteristics (González-Gaitán et al. 2011; Maguire et al. 2011; Sullivan et al. 2011). The normal template was constructed with a large sample of SNe Ia at low and high redshift, whereas the 91bg-like SN Ia template comes from the classical subluminous SN 1991bg and SN 1999by. Although there are many more 91bg-like SNe Ia at present to improve this template, we show in the following that it is appropriate for our purposes.

[8] http://supernova.lbl.gov/nugent/nugent_templates.html

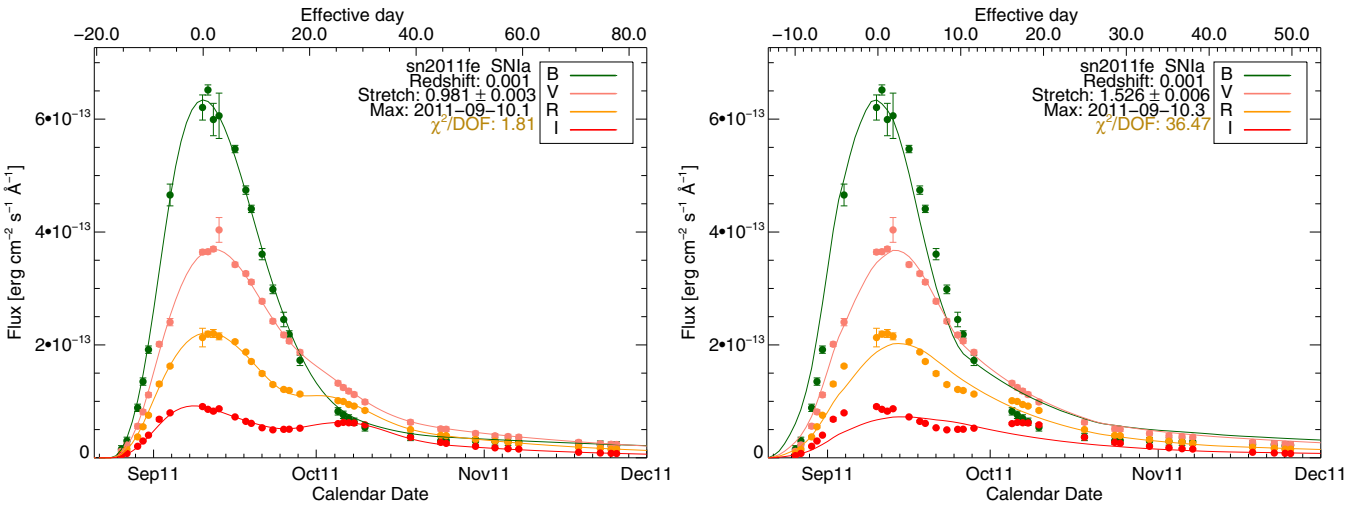

Figure 1. Example SiFTO light curve fits of SNe Ia with better normal (left) than 91bg-like (right) Ia template fits. SN 2011fe has $s_{\rm Ia} = 0.98$, $\chi^2_\nu({\rm Ia}) = 1.8$, and $\chi^2_\nu(91{\rm bg}) = 36.5$.

(A color version of this figure is available in the online journal.)

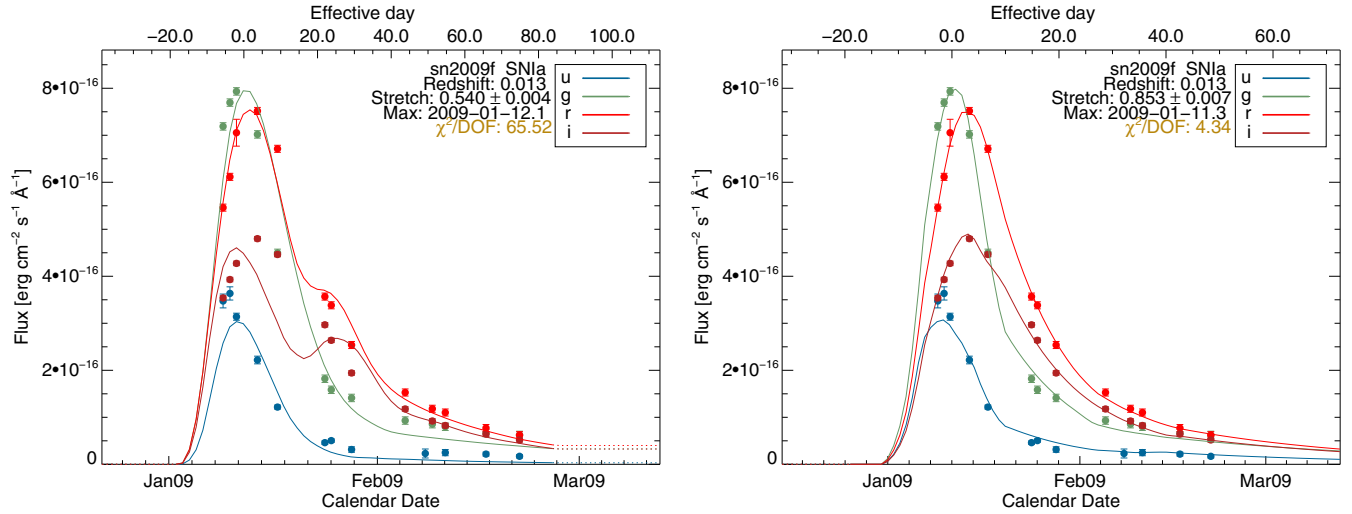

Figure 2. Example SiFTO light curve fits with worse normal (left) than 91bg-like (right) Ia template fits. SN 2009F has $s_{\rm Ia} = 0.54$ ($s_{91{\rm bg}} = 0.85$), $\chi^2_\nu({\rm Ia}) = 65.6$, and $\chi^2_\nu(91{\rm bg}) = 4.3$.

(A color version of this figure is available in the online journal.)

In order to ensure a proper fit, we require at least two filters, each with at least one data point between −15 and 0 days and one between 0 and 25 days past the *B*-band maximum. We perform fits using all available optical photometry down to 85 days past maximum. If different photometric calibrations from different instruments exist per filter set, we choose only one set, based on the number of data points, to ensure consistent photometry per filter. Ideally, as will be shown later, red bands such as *R* or *r* and *I* or *i* are beneficial to fully exploit the range of possible SN Ia sub-groups. The SiFTO fits are performed with both "normal" and "91bg" templates. Some example fits are shown in Figures 1 and 2, where one can compare the quality of the fits for the two templates for two SNe Ia: SN 2011fe and SN 2009F. The first presents better normal template fits as seen in the figure as well as on the lower overall reduced fit quality, $\chi^2_\nu({\rm Ia}) < \chi^2_\nu(91{\rm bg})$, whereas the other shows better 91bg template fits and has $\chi^2_\nu({\rm Ia}) > \chi^2_\nu(91{\rm bg})$. We first use this simple photometric criterion (criterion 1) to separate the SN Ia population into photometric normal and SN 1991bg/SN 1999by-like objects. We note that for fits with a 91bg template, a "stretch" has a different meaning since it is with respect to a typical 91bg-like SN Ia, so SN 1991bg and SN 1999by have a "normal template" stretch of $s_{\rm Ia} = 0.46$ and 0.62 but a "91bg template" stretch of $s_{91{\rm bg}} = 0.86$ and 1.02, respectively. The definition of standard $s = 1$ SN is shifted in both cases. We also emphasize that the stretch parameter is a factor defined in the *B* band, so that it best evaluates the variation near this wavelength.

2.3. Blue- and Red-band Template Fits

Although the 91bg-like SN Ia classifying technique based on the overall χ^2_ν comparison between normal and 91bg template fits is quite good at separating 91bg-like from normal SNe Ia according to spectroscopic classifiers, as will be shown in next sections, there is a fraction of non-91bg-like objects that are classified as such. Closely investigating these objects, we find that many of them are actually peculiar SNe Ia of a different kind. SNe Iax are all classified as 91bg-like SNe Ia, super-Chandrasekhar objects as well, and even SN 2013bh, the only other 2000cx-like member in the literature (Silverman et al. 2013b) is also included. Although intriguing at first, one can

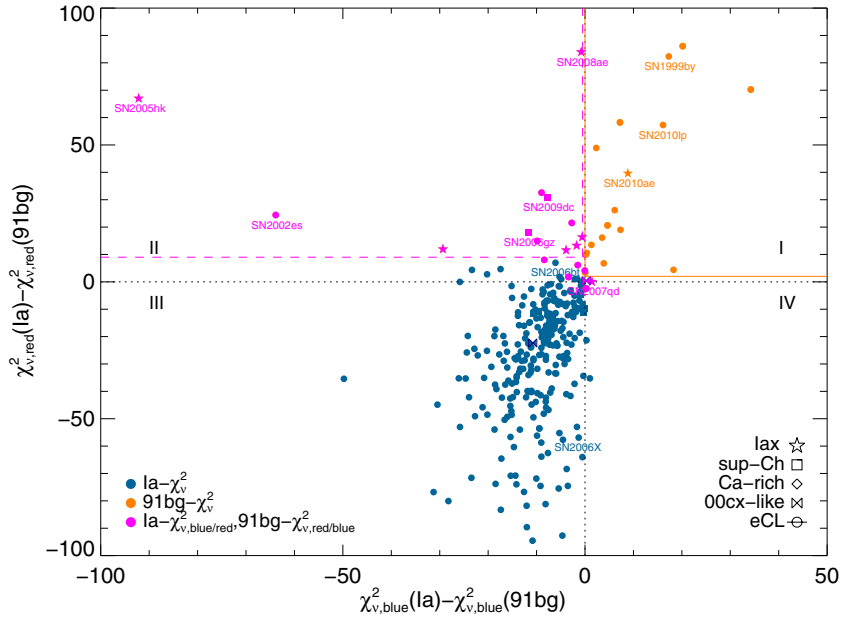

Figure 3. Difference between normal and 91bg template fit qualities in the blue bands (U/u, B and g): $\chi^2_{\nu,\mathrm{blue}}(\mathrm{Ia}) - \chi^2_{\nu,\mathrm{blue}}(91\mathrm{bg})$ vs. the difference between normal and 91bg template fit qualities in the red bands (V, R/r and I/i): $\chi^2_{\nu,\mathrm{red}}(\mathrm{Ia}) - \chi^2_{\nu,\mathrm{red}}(91\mathrm{bg})$. Zero χ^2_ν difference dotted lines are shown and solid orange lines denote the maximum FoM(91bg) box (or quadrant I) of 91bg-like objects according to both criteria, the overall and blue-/red-band fits. The blue symbols represent normal photometric candidates, where the overall fits are consistent with a normal SN Ia template. The orange symbols are 91bg-like candidates according to both criteria (overall, blue-, and red-band) fits that are delimited by the orange box. The purple symbols are objects that are 91bg-like according to the overall fit (criterion 1), but not according to criterion 2 of blue-/red-band fits, i.e., they lie outside of the orange box. A box of minimum FoM(pec) is shown as purple dashed lines, although it is not used as part of the classification. Different symbol shapes show known peculiar or extreme objects such as SNe Iax (stars), super-Chandrasekhar SNe Ia (squares), and SN 2000cx-like objects (bowtie) and extremely cool SNe Ia or "eCL" (circles with horizontal lines) as in Folatelli et al. (2013).

(A color version of this figure is available in the online journal.)

understand this result as their light curves in redder bands resemble those of typical 91bg-like objects more than those of normal ones, showing less or no shoulder and secondary maxima.

Nonetheless, one can also see that their photometric behavior is different from the true 91bg-like objects in the bluer bands and that the overall χ^2_ν is being driven by extremely poor normal template fits in the redder bands. To investigate this further, we re-fit our entire sample restricting the fit to "blue-bands," i.e., using the following available filters simultaneously: u or U, B, and g, with both templates, normal and 91bg-like. Then, we do the same but restricting the fit to "red-bands," i.e., simultaneously using filters V, r, or R, and i or I. For this, we require at least one filter with one point prior to maximum and one after maximum. Figure 3 shows the resulting difference in fit quality between the normal and 91bg templates for the red-band versus blue-band fits. We denote four quadrants in this plot, which we will refer to throughout the paper. In this figure, we can see that if we add a restriction to the photometric definition of a 91bg-like SN Ia based on the result of the comparison of fits in the blue and red bands, i.e., $\chi^2_{\nu,\mathrm{blue}}(91\mathrm{bg}) < \chi^2_{\nu,\mathrm{blue}}(\mathrm{Ia})$ and $\chi^2_{\nu,\mathrm{red}}(91\mathrm{bg}) < \chi^2_{\nu,\mathrm{red}}(\mathrm{Ia})$ (vertical and horizontal dotted lines), criterion 2, we discard almost all peculiar SNe Ia, in particular all SNe Iax except for SN 2010ae and SN 2007qd, and all super-Chandrasekhar SNe Ia, while keeping the known spectroscopic 91bg-like SNe Ia. It is worth mentioning that since only two objects have better 91bg template fits in the blue bands but worse in the red bands (quadrant IV), this criterion could also only consist of just a blue-band selection and no red-band selection to include most objects.

The separation between these groups does not necessarily need to be at exactly $\chi^2_{\nu,\mathrm{blue}}(91\mathrm{bg}) = \chi^2_{\nu,\mathrm{blue}}(\mathrm{Ia})$, and $\chi^2_{\nu,\mathrm{red}}(91\mathrm{bg}) = \chi^2_{\nu,\mathrm{red}}(\mathrm{Ia})$ (dotted lines in Figure 3), and could instead be offset from these lines. To investigate this further, we use a common photometric classifying diagnostic (e.g., Kessler et al. 2010b), the Figure of Merit (FoM), given by the efficiency of the classification (ϵ), i.e., the fraction objects of a given type correctly tagged, and the purity (P) or fraction of classified objects that really are of that type, i.e., a measure of the false positive tags:

$$\mathrm{FoM} = \epsilon \times P = \frac{N^{\mathrm{true}}}{N^{\mathrm{tot}}} \times \frac{N^{\mathrm{true}}}{N^{\mathrm{true}} + N^{\mathrm{false}}}, \quad (2)$$

where N_{true} is the number of correctly identified objects of a given type (e.g., 91bg-like objects), N_{tot} is the total input number of that type, and N_{false} is the number of objects falsely tagged as objects of that given type.

Calculating this FoM for known 91bg-like objects, FoM(91bg), for different boxes around $\chi^2_{\nu,\mathrm{blue}}(91\mathrm{bg}) - \chi^2_{\nu,\mathrm{blue}}(\mathrm{Ia}) = \pm 20$ and $\chi^2_{\nu,\mathrm{red}}(91\mathrm{bg}) - \chi^2_{\nu,\mathrm{red}}(\mathrm{Ia}) = \pm 20$ and looking for the maximum FoM, we find the areas highlighted in orange in Figure 3. This box is similar to the original $\Delta\chi^2_\nu = 0$ with a slight vertical offset of $\chi^2_{\nu,\mathrm{red}}(\mathrm{Ia}) - \chi^2_{\nu,\mathrm{red}}(91\mathrm{bg}) = 2$, which leaves out peculiar SN 2007qd and SN 2013bh. Objects inside this region, besides having a better overall 91bg template fit, are also 91bg-like candidates according to the blue-/red-band fits (criteria 1 and 2). This selected group is located in quadrant I of the figure and symbols therein are shown in orange. SN 1991bg-like candidates according to the overall $\chi^2_\nu(91\mathrm{bg})$ (criterion 1) that are not in this region, i.e., do not fulfill criterion 2, are denoted with purple symbols in the figure (mostly in quadrant II). Blue symbols are normal candidates according to the overall fit.

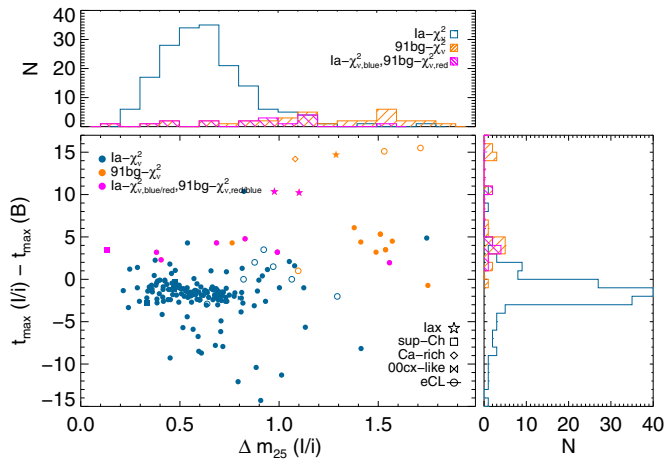

Figure 4. Difference between day of maximum light in the I or i band and maximum in the B band vs. Δm_{25} in the I or i band. SNe with overall fits more consistent with normal template fits are shown as filled blue symbols. Objects that have better overall 91bg template fits (fufilling criterion 1) and better blue-/red-band 91bg template fits (fulfilling criterion 2) are shown in orange, whereas those with better overall 91bg template fits yet better blue-/red-band normal template fits are shown in purple. Symbols represent known peculiar or extreme objects: Iax (stars), super-Chandra (square), Ca-rich (diamond), 00cx-like (bowtie), and eCL (circles with line). Additionally, objects for which not enough data was available to check the blue- and red-band fits are shown as open symbols for photometric normal (blue) and 91bg-like (orange) SNe Ia. The upper and right panels show the distributions for both samples in empty blue and filled orange boxes, respectively.

(A color version of this figure is available in the online journal.)

Alternatively, to eliminate the first criterion and to be able to select peculiar SNe Ia, i.e., those objects in purple, one can also find a region of maximum FoM(pec) in a similar fashion to FoM(91bg). This results in the area shown in purple dashed lines. This zone, however, does not include the two objects in quadrant IV, SN 2007qd and SN 2013bh. These dividing lines are sensitive to the training sample used and will therefore be studied in more detail in Section 4.

2.4. Comparison with Other Light Curve Parameters

In the examples shown in Figures 1 and 2, it seems evident that the shoulder and secondary maxima of bands at longer wavelengths determine the quality of the fits since they are present in normal SNe Ia as opposed to 91bg-like objects. Nevertheless, it is important to note that the time of maximum in each band also plays a crucial role. To test these light curve characteristics independently from SiFTO, we calculate the time of maximum in each band using a fourth degree polynomial fit and we also look for a secondary maximum with another polynomial fit. If the secondary maximum is not very separated in time from the primary maximum in redder bands such as R/r or I/i, we are not able to define such a secondary; in fact, we find a secondary maximum in I/i for only 2 (of 48) 91bg-like candidates according to criterion 1, whereas this is found for more than 90 (of 295) normal SNe Ia. A more continuous parameter that can be defined for a larger sample is the magnitude change after 25 days past maximum or Δm_{25}: if an SN has a secondary shoulder or a maximum that typically occurs 20–35 days past maximum for redder bands, then this parameter should somewhat reflect this. In Figure 4, we show two light curve diagnostics, the difference in the maximum between two different bands, $t_{max}(B) - t_{max}(I/i)$ and $\Delta m_{25}(I/i)$, for the samples selected with the mechanism shown in the previous section. Clearly, as expected, the normal SNe Ia according to our light curve fits have maxima in red bands that occur earlier and they also have lower $\Delta m_{25}(I/i)$ than 91bg-like candidates that had better overall, blue, and red-band 91bg template fits (filled orange). Objects with better overall but worse blue/red 91bg template fits (filled purple) also differ from normal SN Ia candidates, although not as strongly as 91bg-like candidates. These trends occur in R/r, are stronger in I/i, and are exacerbated in the NIR (Phillips 2012).

2.5. Comparison with Spectral Classificators

The standard classification of supernovae is defined by identifying spectral features near maximum light. Several classification schemes for SNe Ia have been proposed, notably those by Benetti et al. (2005), Branch et al. (2006), and Wang et al. (2009a), all based on prominent line properties such as Silicon strength, velocity, and velocity gradient. Additionally, some automated classification tools such as SNID (Blondin & Tonry 2007) or GELATO[9] (Harutyunyan et al. 2008) have been presented for general use.

Using a large sample of classifications from SNID given by Silverman et al. (2012), we compare them to our photometric classificator. 220 SNe Ia match their sample and we show the result in Figure 5. SNID gives the following classifications for SNe Ia: Ia-norm, Ia-91T, Ia-91bg, Ia-CSM, Ia-99aa, and Ia-02cx. We group here Ia-91T, Ia-99aa, and Ia-CSM together into a single bin that, as can be seen, has no further influence in our classification. From this figure, one can see that most of the 187 objects (99.5%) photometrically classified as normal SNe Ia are also normal according to SNID. On the other hand, we do see that photometric 91bg-like candidates are found in other bins. In particular, seven objects leak into the Ia-norm bin. Some of these objects, like SN 2007on, are borderline between photometric normal and 91bg-like according to our overall fits having very similar χ^2_ν, but some others have quite interesting properties that make them stand out, like super-Chandrasekhar SNe Ia. Most of these can be identified with quality of fit in particular filter sets, as shown in the last section, and shown in the figure with purple histograms. All SNe Iax are classified as photometric 91bg-like SNe Ia according to the overall fit. This result is possibly physically interesting per se, and for cosmological studies seeking for purely normal SNe Ia, it also presents a way to photometrically classify more than one group of peculiar objects simultaneously. For a 91bg-like SN Ia classification technique, however, this could be worrisome. Fortunately, the inclusion of blue-/red-band fits permits us to discriminate quite well between both groups as well.

Blondin et al. (2012) also present a large spectroscopic data set and publish the classifications of Branch et al. (2006) and Wang et al. (2009a) for their sample. We find 189 matches and show the comparison in Figure 5 for these spectral groups. In general, we find agreement with our classifying (the "Cool," CL, group corresponds to the 91bg-like for Branch et al. 2006). We again find that some objects that we classify photometrically as 91bg-like according to the overall fit are misidentified according to these spectral classifications. Nevertheless, most of these actually correspond to SNe Iax and super-Chandrasekhar SNe Ia and are mostly included in the purple histograms that take into account blue-/red-band fits. Thus, from this we see that the technique presented here allows us to differentiate quite successfully between normal, 91bg-like, and other peculiar SNe

[9] Available at https://gelato.tng.iac.es/

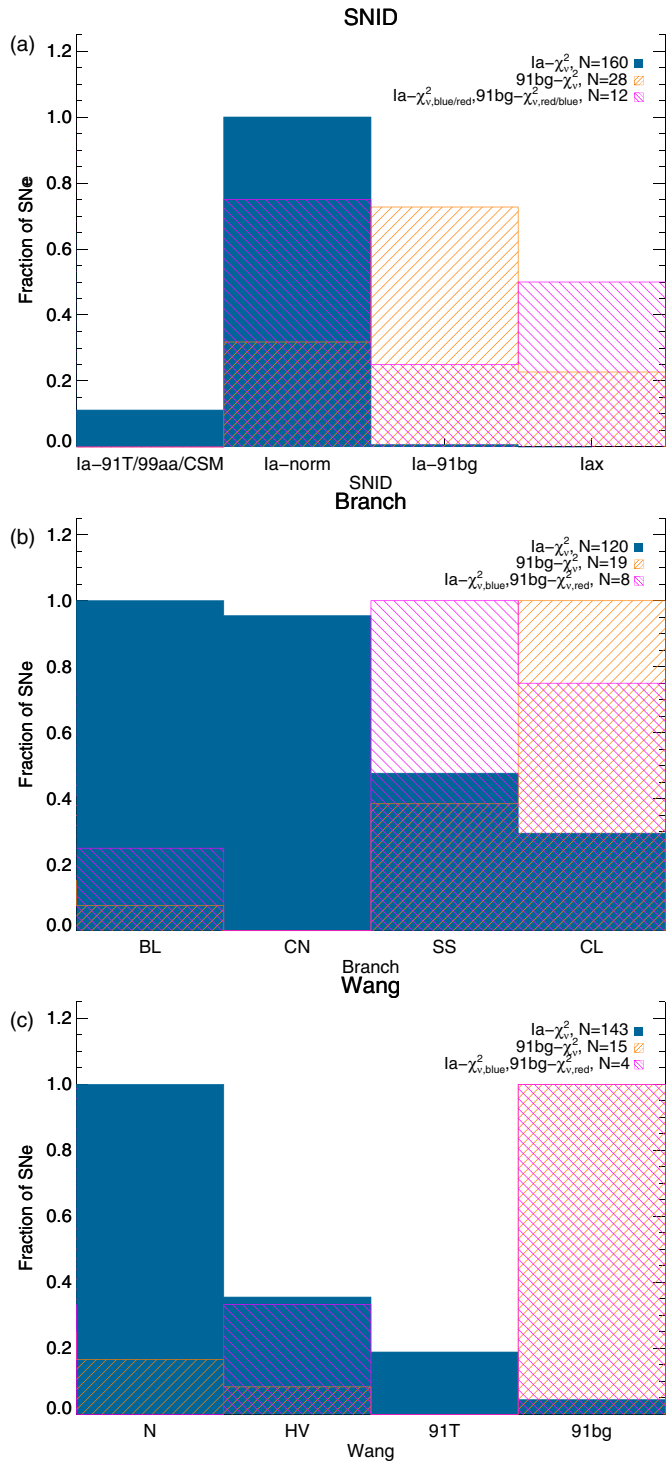

Figure 5. Comparison of the photometric classification technique to detect normal, 91bg-like, and other peculiar SNe Ia with spectral classifiers: (a) SNID (Blondin & Tonry 2007), (b) Branch et al. (2006), and (c) Wang et al. (2009a). Blue histograms (open) show objects with better overall normal template fits, orange (filled with 45° lines) histograms show objects with better overall 91bg template fits and better blue-/red-band 91bg template fits (criteria 1 and 2), whereas purple (filled with −45° lines) are objects with better overall 91bg template fits but worse blue- or red-band 91bg template fits (criterion 1). Histograms are normalized to one and the total number for each histogram is indicated in the figures.

(A color version of this figure is available in the online journal.)

Ia, notably SNe Iax. These other sub-classes will be discussed further in the following sections.

In general, we find a remarkable agreement between our photometric classification and the different spectroscopic classifiers. This is impressive given that SiFTO was not originally devised for this purpose and it opens up promising possibilities for other transient surveys.

3. RESULTS

We explore in Figure 6 the range of parameters obtained with our fits comparing SiFTO color $\mathcal{C}$ with stretch s obtained with both templates: normal and 91bg-like. Since SiFTO fits every filter flux scale independently, both colors, measured with normal and 91bg templates, should, in principle, be comparable. For stretch, on the other hand, since a $s = 1$ has different meanings in both cases, the values will be quite different but the stretches should be correlated. We indeed find the following relation for stretch: $s_{\mathrm{Ia}} = (1.676 \pm 0.001) \times s_{91\mathrm{bg}} - (0.082 \pm 0.002)$ with rms $= 0.16$; and for color: $\mathcal{C}_{\mathrm{Ia}} = (1.007 \pm 0.003) \times \mathcal{C}_{91\mathrm{bg}} - (0.040 \pm 0.001)$ with rms $= 0.06$. The parameters one should use are defined by the fit quality; e.g., if an object has a better 91bg template fit, one should use the parameters obtained with the 91bg template fit, and vice versa.

We also show the magnitude–stretch and magnitude–color obtained with SIFTO from the 91bg template fits in Figure 7. These magnitudes are only corrected for distance assuming a standard cosmology for SNe in the Hubble flow ($z > 0.01$) or different estimates from the NASA/IPAC Extragalactic Database (NED) when closer. We can see that most of SNe Ia, including normal and 91bg-like, follow a narrow trend of magnitude versus color, regardless of the nature of the color: intrinsic or reddened. Some SNe Iax are the only exception being very faint for their colors. The different aspects of the SN Ia sub-groups shown in these figures will be developed further in the following sections.

3.1. SN 1991bg-like SNe Ia

We now focus on the SN 1991bg-like sample defined as objects with better overall blue and red 91bg template fits (orange box in Figure 3), which represent the classical objects similar to SN 1991bg. In both panels of Figure 6, we can see that this group spans the shortest stretch range, between $s_{\mathrm{Ia}} \simeq 0.4$–$0.75$ (or $s_{91\mathrm{bg}} \simeq 0.7$–$1.1$). However, we note that a cut based solely on normal stretch, as done in previous studies, would be insufficient to define classical 91bg-like SNe Ia photometrically. Some SNe Ia like SN 2008R have a fast evolving light curve, i.e., low stretch, but are better fit with a normal SN Ia template. Some normal low-stretch SNe Ia do exist and are characterized for having bluer colors than normal SNe Ia. Therefore, a color cut would also be needed to ensure an almost uncontaminated population. Using a color cut of $\mathcal{C}_{\mathrm{Ia}} > 0.3$ (or $\mathcal{C}_{91\mathrm{bg}} > 0.2$) and a stretch cut of $s_{\mathrm{Ia}} < 0.72$ (or $s_{91\mathrm{bg}} < 1.08$) (shown with dashed lines in Figure 6) instead of the above χ^2 criteria, we recover most of the real 91bg-like candidates, leaving out all other SNe Ia except for two SNe Iax of very low stretch. Using exclusively a cut with the 91bg stretch, $s_{91\mathrm{bg}} < 1.08$, is a better discriminator that almost does not require the extra color cut needed when using the normal stretch. We note that a potential problem of a simple color and stretch cut instead of our χ^2 fit analysis would be the presence of

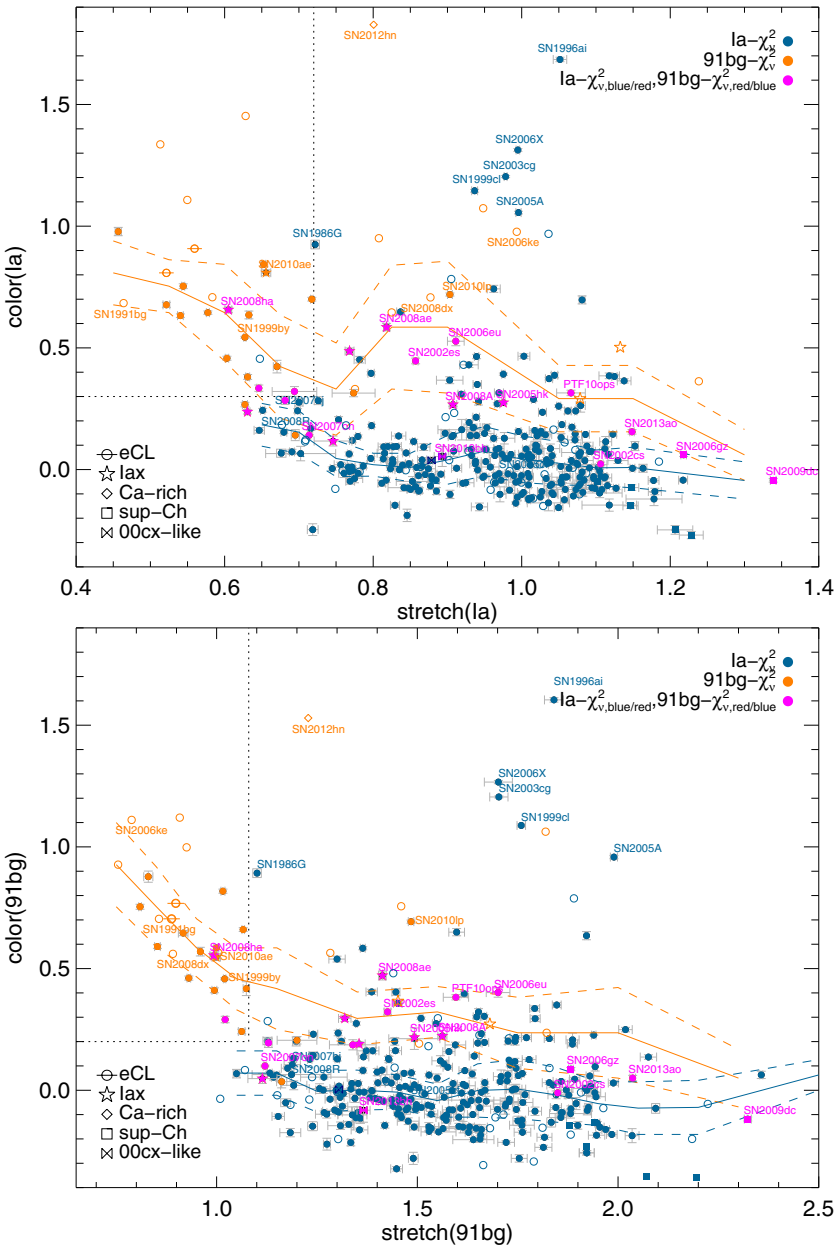

Figure 6. (a) SiFTO colors vs. stretch for the normal template fits (top), and (b) 91bg template fits (bottom). Same symbols and colors as in Figure 4. The solid lines represent the median of the photometric normal (91bg-like) sample in blue (orange) according to only the overall fits (criterion 1). The dashed lines are the standard deviation on the median for both samples. The vertical and horizontal dotted lines denote the 91bg-like SN Ia region.

(A color version of this figure is available in the online journal.)

highly reddened normal SNe Ia at low stretch mimicking typical 91bg-like SNe Ia.

It is worth mentioning that the transition region between photometric normal and 91bg-like objects is well populated in both Figures 3 and 6(a), with no evidence of a clear gap, as hinted in Phillips (2012). The few 91bg-like objects found in the normal defined region have very similar χ^2_ν for both templates. This is the case for SN 2007on, for example, a photometric 91bg-like SN Ia with a very similar fit quality with a normal template. On the other hand, SN 2007hj is a photometrically normal SN Ia with basically the same fit quality with both templates. In fact, there are in total eight objects with $|\chi^2_\nu(\mathrm{Ia}) - \chi^2_\nu(91\mathrm{bg})| < 1$, five of which lie in the transition region, i.e., $0.68 < s_{\mathrm{Ia}} < 0.80$. Other examples include SN 1986G, a low-stretch ($s_{\mathrm{Ia}} = 0.72$), highly reddened from extinction in the host galaxy. This SN has slightly better normal template fits with indications of shoulder and secondary maxima in the red bands. This is ultimately confirmed through NIR observations (Phillips 2012). These transition objects hint toward a smooth transition from 91bg-like to normal SNe Ia. Nonetheless, one can arguably see a slight gap in the color-stretch figure for the 91bg template (Figure 6(b)) and the behavior of the 91bg-like sample for the color–stretch relations, as well as for the relations between magnitude–stretch (see Figure 7(a)) present different slopes than for the normal population. We will investigate this issue further with a cluster analysis in Section 4.5.1.

Folatelli et al. (2013) define an "extreme cool" (eCL) spectroscopic sample based on the pseudo-equivalent width of the Mg II line complex around 4300Å, which includes Ti II lines. The more extreme 91bg-like objects have the strongest features

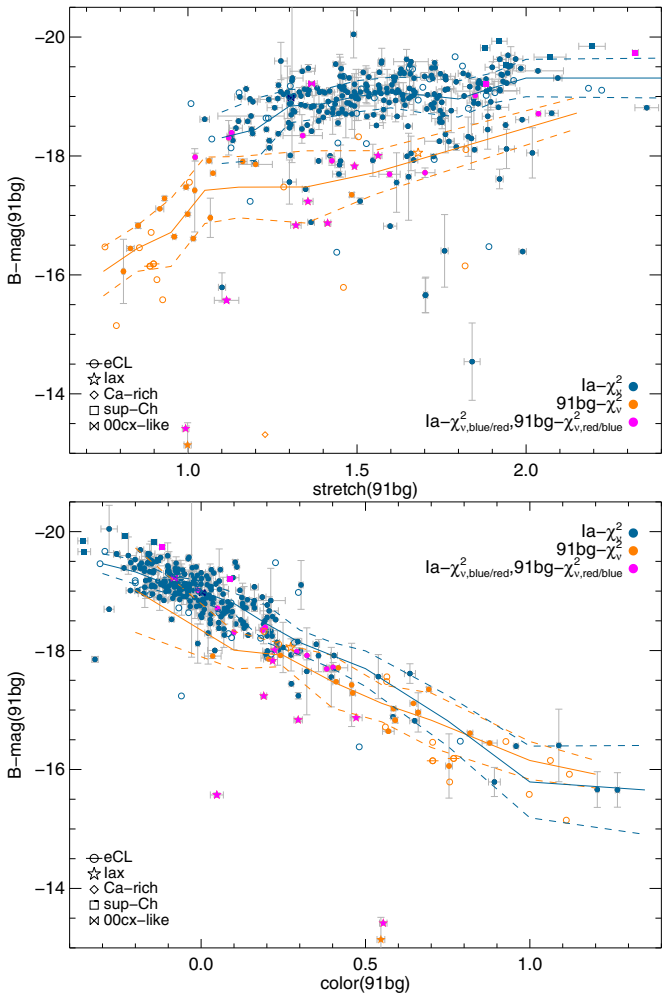

Figure 7. (a) SiFTO *B*-magnitude vs. stretch (top), and (b) SiFTO *B*-magnitude vs. color (bottom) for 91bg template fits. Magnitudes are corrected for distance and MW extinction. Same symbols and colors as in Figure 4. Solid lines show the median of the photometric normal (91bg) sample in blue (orange) according to only the overall template fits (criterion 1). Dashed lines are the respective standard deviation on the mean.

(A color version of this figure is available in the online journal.)

and are therefore eCL objects. We identify those objects in our figures and we note that, as expected, they have the largest χ^2_ν difference between normal and 91bg template fits, giving further evidence of the power of this technique.

Finally, it is worth noting that two objects, SN 2006ke and SN 2008dx, spectroscopically classified as SN 1991bg-like with SNID in Silverman et al. (2012) and which we identify as 91bg-like candidates according to the overall fit (but we do not have sufficient data in the blue bands to confirm them) lie in the proper region defined in the upper left of Figure 6 for the 91bg fits (6b) but not for the normal fits (6a). This confirms that one should use the parameters obtained with the best template.

3.2. Slowly Evolving SN 1991bg-like SNe Ia

The present study has revealed that many peculiar SNe Ia bear some light curve similarities with typical 91bg-like SNe Ia and that they are classified as such with a simple single criterion. The clearest example of this are the high-stretch 91bg-like SNe Ia: PTF 10ops (Maguire et al. 2011) and SN 2010lp (G. Pignata (2014, in preparation; Kromer et al. 2013b), which have wide light curves, yet 91bg-like spectra and red colors. This set of objects is classified as 91bg-like according to criterion 1 of our photometric method: they have better overall light curve fits with a 91bg template. Furthermore, SN 2010lp has both blue- and red-band fits that are better with a 91bg template (criterion 2) as well. For PTF 10ops, there is only one blue band, g' filter, with a few data points and whose fit is $\chi^2_{\nu,\mathrm{blue}}(\mathrm{Ia}) = 0.36$ vs. $\chi^2_{\nu,\mathrm{blue}}(91\mathrm{bg}) = 0.40$, which are basically identical, so it is difficult to distinguish between a peculiar SN Ia such as SN 2002cx or a high-stretch 91bg-like SN Ia. However, if we take into account the region denoted in purple in quadrant II of Figure 3 as a delimiter of SNe Iax, and we include the purple dots below as possible 91bg-like objects, we add three more SNe Ia to the 91bg-like objects: PTF 10ops, SN 2006eu, and SN 2007ba. The latter one is a transitional object with $s_{91\mathrm{bg}} = 1.13$ ($s_{\mathrm{Ia}} = 0.68$), for which SNID gives a 91bg-like classification. SN 2006eu is a higher-stretch object ($s_{\mathrm{Ia}} = 0.91$,$s_{91\mathrm{bg}} = 1.70$) with a normal SNID classification; the CfA classification,[10] however, signals its similarity to a 91bg-like object. Another object, SN 1999bh with $s_{91\mathrm{bg}} = 1.46$ and $\mathcal{C} = 0.76$, is classified as 91bg-like according to the overall fits but there is not enough pre-maximum data in the blue available to study it further. SNID, however, gives 91bg-like matches, making this SN another potential member of this group, although it also finds some matches to SN 2006bt (see Section 3.5). Ganeshalingam et al. (2012) also mention the peculiarity of this object. This would imply that we identify three to four high-stretch SNe with photometric 91bg-like characteristics according to criteria 1 and 2. No other similar SNe Ia are known in the low-z literature, suggesting that they are rare or that they occur in remote regions (Maguire et al. 2011) and have therefore been overlooked in historic galaxy targeted surveys.

3.3. Type Iax Supernovae

An important outcome of the initial overall χ^2_ν comparison of the fits with the two different templates is the identification of all 10 SNe Iax in the literature that pass the light curve cuts. Including then the blue- and red-band χ^2_ν comparison, we can differentiate between real 91bg-like objects and the remaining seven SNe Iax after the new cuts, with the exception of SN 2010ae, which has better 91bg template fits in all cases as well as a low stretch. So, from a photometric perspective, SNe Iax appear as a mixture between normal and 91bg-like SNe Ia: they have a blue-band behavior that is more similar to standard SNe Ia, but have red-band light curves much more similar to 91bg-like SNe Ia. In Figure 8, we show SN 2005hk as an example of all four fits: blue-band and red-band fits for normal and 91bg templates. One can see that although the blue-band fit agrees more with a normal template, the fit is far from perfect. This behavior is found in other SNe Iax, even when only one blue filter is available, like for SN 2002cx. Even with the use of templates that were not designed for SNe Iax, we are able to identify them quite well.

SN 2010ae is an extreme of the SN Iax population (Stritzinger et al. 2014) with very low stretch but also red colors. The difference in χ^2_ν for both templates is also quite large for the blue-band fits. This is a striking result given that SN 2008ha, another extreme case of the population, falls into the SN Iax category through the blue-band fits. Both, however, are very faint (even taking into account extinction; see Stritzinger et al. 2014), far off the classical 91bg-like population, as shown in Figure 7, so they can be easily identified. Two more SNe Iax, SN 2011ay and SN 2012Z, are photometrically identified as

[10] http://www.cfa.harvard.edu/supernova/RecentSN.html

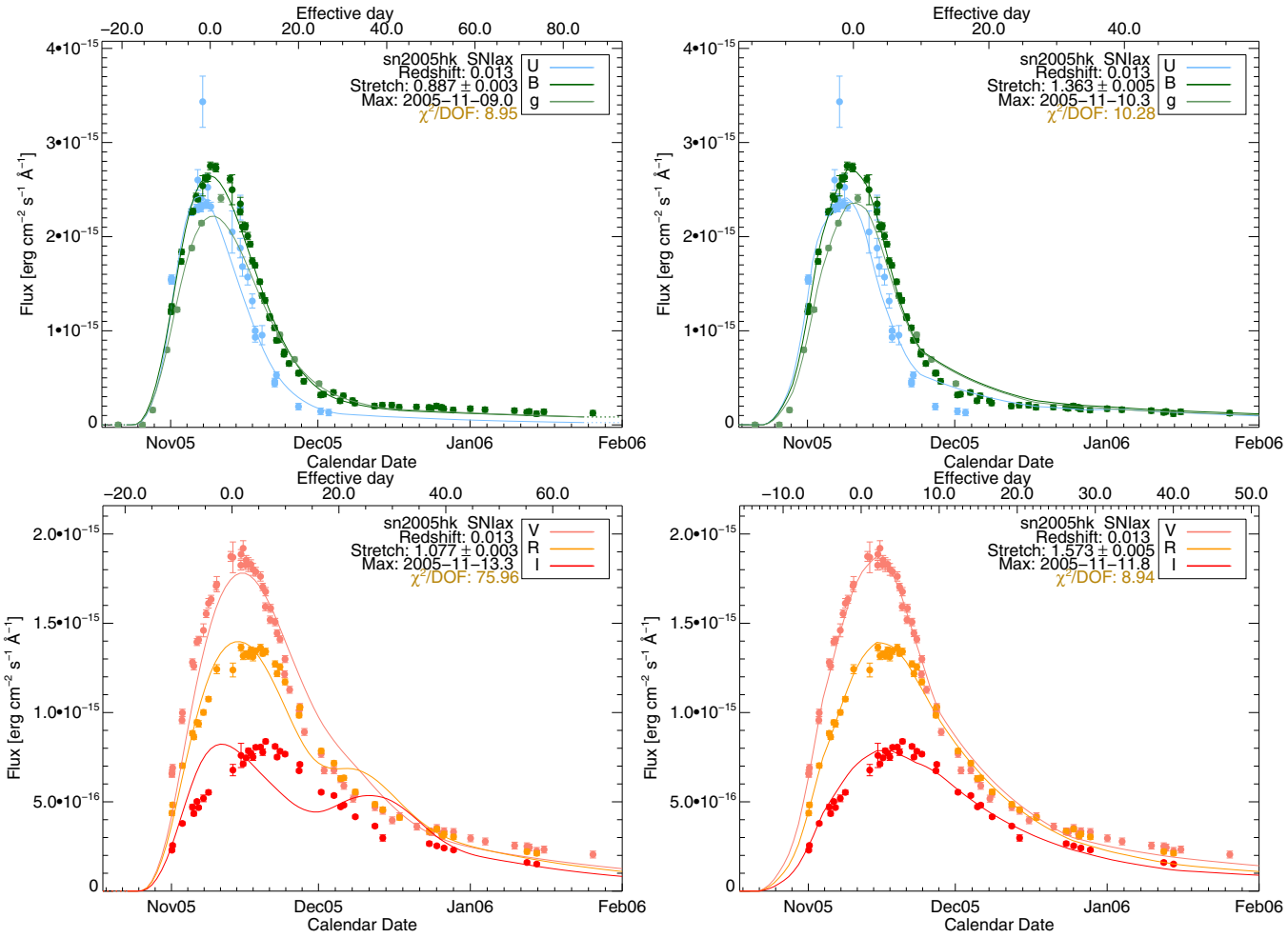

Figure 8. SiFTO fits to the light curve of SN 2005hk with a normal SN Ia template (left) and with a 91bg SN Ia template (right) using exclusively blue bands (upper) and red bands (lower).

(A color version of this figure is available in the online journal.)

91bg-like candidates with criterion 1 but there is not enough data in the blue bands to evaluate criterion 2.

On the other hand, we find another candidate that is not classified as SN Iax in the literature: SN 2002es. Classifying it with SNID, we find that it is a 91bg-like object with $s_{\rm Ia} = 0.86$ and $s_{\rm 91bg} = 1.43$; no match to any SN Iax is found. Ganeshalingam et al. (2012) note the peculiarity of this object and discuss the similarities to 91bg-like and to 02cx-like objects. Therefore, it seems that this object might be in between SNe Iax and slowly evolving 91bg-like objects, such as PTF 10ops. Alternatively, it could make up part of another similarly peculiar group, SN 2006bt-like objects, which will be discussed later. White et al. (2014) reach a similar conclusion in which both SN 2002es-like SNe and SNe Iax have common spectroscopic and photometric properties, although SN 2002es-like objects have more pronounced Ti II features, characteristic of 91bg-like objects.

3.4. Super-Chandrasekhar SNe Ia

Besides SNe Iax, another eight SNe Ia have better overall and worse blue- or red-band 91bg template fits. Two of those catch our attention: SN 2006gz and SN 2009dc. These two supernovae are super-Chandrasekhar SN Ia candidates (e.g., Hicken et al. 2007; Maeda et al. 2009; Taubenberger et al. 2011; Hachinger et al. 2012; Kamiya et al. 2012). Taking a closer look at their light curves, one can understand why this occurs: the red-band part is better fit with the 91bg template. Since super-Chandrasekhar SNe Ia have characteristic $I - /i$-band light curves where the secondary maximum occurs earlier than for normal SNe Ia, the two maxima merge and create an almost plateau with a unique elongated maximum. SN 1991bg-like SNe Ia also have only one maximum, which, even of shorter duration, can better approximate super-Chandrasekhar light curves. The same occurs in the R/r band where the shoulder of super-Chandrasekhar almost disappears, simulating the behavior of 91bg-like objects (see Figure 9). Investigating the classical super-Chandrasekhar SN 2003fg (Howell et al. 2006), which was not originally included in our analysis due to its higher redshift ($z = 0.24$), we find that it is also better fit with a 91bg template for the overall, but also the blue- and red-band light curves. However, given its high stretch ($s_{\rm 91bg} = 1.99$, $s_{\rm Ia} = 1.30$), one can easily tell it apart from regular 91bg-like and PTF 10ops-like objects. SN 2007if (Scalzo et al. 2010), on the other hand, does not have pre-maximum data to perform our analysis. In addition to these supernovae, Scalzo et al. (2012) present five super-Chandrasekhar candidates. Our technique does not select these at all. This is due to their wider definition which is more similar to typical SN 1991T-like objects. One can indeed see that these light curves have clearly distinct secondary maxima in I/i and definite shoulders in R/r. Our

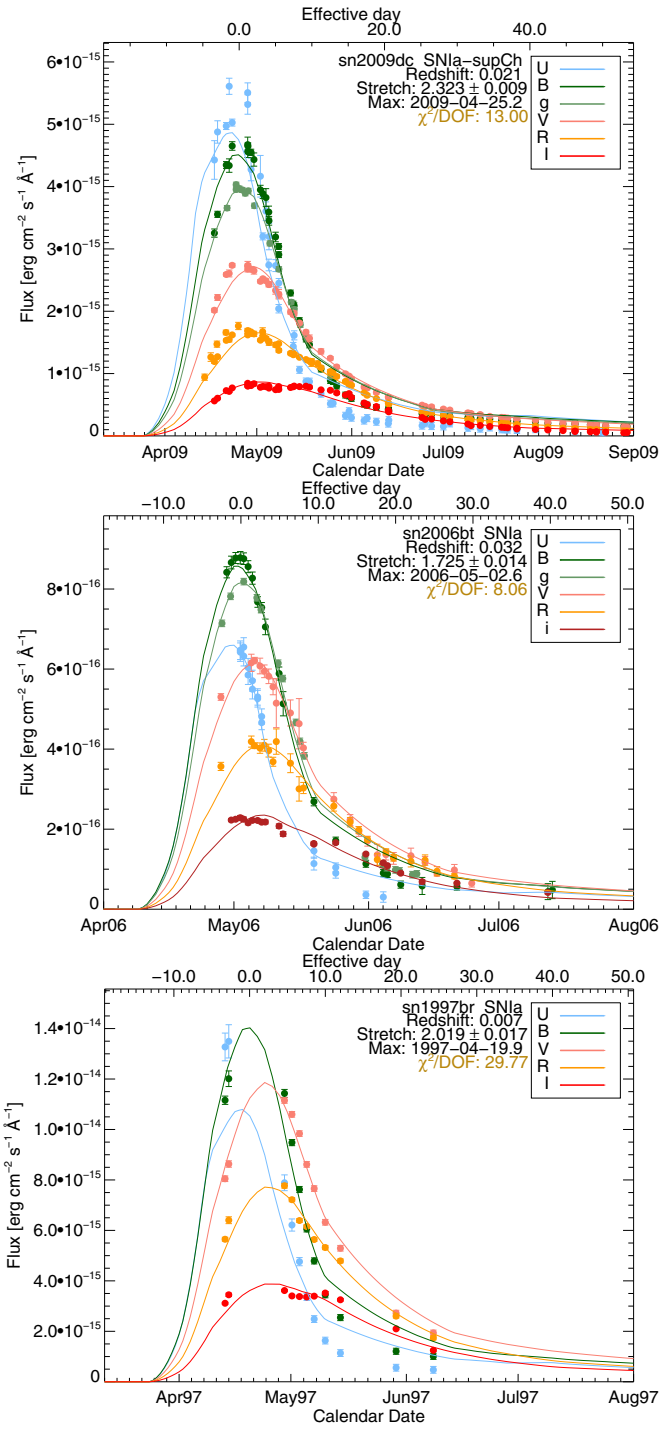

Figure 9. SiFTO fits to the light curves of SN 2009dc, SN 2006bt, and SN 1997br with a 91bg SN Ia template.

(A color version of this figure is available in the online journal.)

method suggests that only the most extreme cases, the standard super-Chandrasekhar SNe Ia, have photometric similarities to other sub-classes as 91bg-like and SN Iax objects.

This method then seems to be capable of also distinguishing super-Chandrasekhar objects. How can one separate them from SNe Iax since they are all identified in the same manner? When one looks at the stretch of these objects, they are beyond $s_{91\mathrm{bg}} > 1.8$ ($s_{\mathrm{Ia}} > 1.2$). Some super-Chandrasekhar candidates identified by Scalzo et al. (2012) have such wide light curves, but, interestingly, their colors are bluer ($\mathcal{C} < -0.12$) as opposed to SN 2006gz ($\mathcal{C} = 0.06$) and SN 2009dc ($\mathcal{C} = -0.05$). SNe Iax, on the contrary, all have $s_{91\mathrm{bg}} < 1.6$ ($s_{\mathrm{Ia}} < 1.05$). As is the case for 91bg-like objects (Section 3.1), this division is clearest with the 91bg instead of the normal stretch.

Another interesting object, SN 2002cs, is identified with our method in a similar way to the super-Chandrasekhar candidates. It also has high stretch, $s_{91\mathrm{bg}} = 2.04$ ($s_{\mathrm{Ia}} = 1.15$), red color ($\mathcal{C} = 0.16$), and it shows small shoulders instead of a secondary maximum in the i-band light curve and no r-band shoulder at all. It is better fit in the red with a 91bg template but not in the blue. However, it is not as bright as typical super-Chandra ($\mathrm{mag}_B = -19.05$). An additional tentative super-Chandra candidate, SN 2009li, at $s_{91\mathrm{bg}} = 1.82$ ($s_{\mathrm{Ia}} = 1.24$), $\mathcal{C} = -0.15$, and $\mathrm{mag}_B = 19.93$, did not have enough data to probe only the blue bands.

3.5. SN 2006bt-like Objects

Some of the objects presented in the previous sections, like the latter super-Chandrasekhar candidate, SN 2002cs, are reminiscent of the peculiar SN Ia presented by Foley et al. (2010b), SN 2006bt. SN 2006bt has spectra similar to 91bg-like SNe Ia, red colors, no prominent secondary maxima, and it occurred in an early-type galaxy, yet it has a slowly declining light curve. Taking a look at the fits of this SN, we see that although the overall fit is better with a normal template, the red-band part is better fit with a 91bg template. In fact, there are several objects for which the overall fit is better with a normal template, but the red-band part is consistent with the 91bg template. All these objects are shown in blue in quadrant II of Figure 3, as opposed to most SNe Iax and super-Chandrasekhar that, with better overall 91bg templates fit, are also in that same quadrant but in purple. Investigating these nine objects, we find that four of them (SN 1986G, SN 2002dl, SN 2007fr, and SN 2007hj), with $0.68 < s_{\mathrm{Ia}} < 0.72$ ($1.05 < s_{91\mathrm{bg}} < 1.20$), are transitional objects between classical 91bg-like and normal SNe Ia. In fact, their spectra do have some SNID matches to 91bg-like objects, as does the CfA classification. On the other hand, the other five objects (SN 1981D, SN 1989A, SN 1997br, SN 2001bf, and SN 2006bt) have higher stretch $0.9 < s_{\mathrm{Ia}} < 1.1$ ($1.4 < s_{91\mathrm{bg}} < 2.0$) and red colors ($\mathcal{C} > 0$). Of these SNe, the last three have sufficient coverage in R/r and/or I/i to inspect the behavior more closely: SN 2001bf has a secondary maximum too close to the first maximum in the I band, SN 1997br shows the maximum much earlier almost forming a single elongated plateau with the first maximum, whereas for SN 2006bt this plateau is almost gone (see Figure 9).

This means that from the light curve behavior perspective, super-Chandrasekhar SNe Ia and these 06bt-like SNe Ia may form the same family resulting from those where the two maxima join in a long plateau in the red bands, including typical super-Chandrasekhar SN 2006gz and SN 2009dc, and also SN 2002cs; then there is a transition of steeper and shorter plateau durations with SN 2006bt, to finish up with SNe Ia that show a weak or very early secondary maximum like SN 1997br and SN 2001bf. The last two are more similar to normal SNe Ia and could be a link between super-Chandrasekhar and normal SNe Ia. In particular, SN 2001bf is not as red as the previous objects. Finally, it is interesting noting that SNID gives a normal Ia classification to SN 2001bf, a 91T-like classification to SN 1997br, and some matches to SN 2006bt are consistent with SN 1986G. This validates that the wide variety of objects that we find to be photometrically similar are partly spectroscopically similar as well.

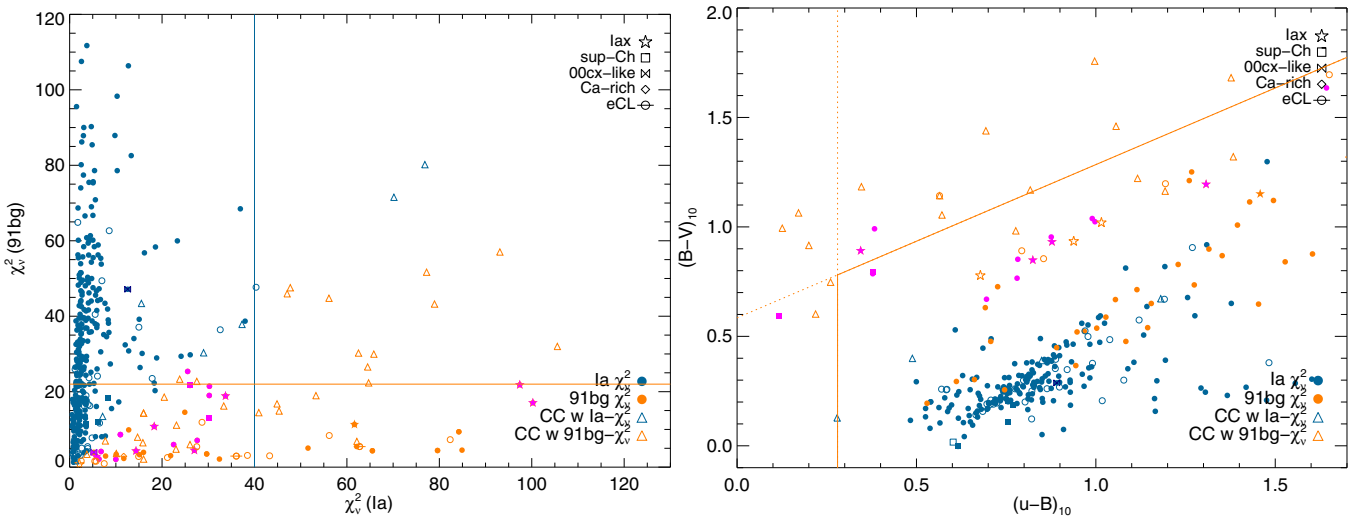

Figure 10. Comparison of the fit quality for the normal template vs. the fit quality for the 91bg template (left) and $B - V$ vs. $u - B$ color diagram at 10 days past maximum (right) for all SNe Ia (same symbols as Figure 4) and for CC SNe shown as blue and orange triangles when better normal and 91bg template fits were achieved. The dividing lines serve as selection criteria against CC contamination.

(A color version of this figure is available in the online journal.)

Finally, the possible high-stretch 91bg-like candidate found in Section 3.3, SN 2002es, has several interesting spectroscopic matches to SN 2009dc according to GELATO, whereas the one found in Section 3.2, SN 1999bh, has SNID matches to SN 2006bt, making them other potential members of the 06bt-like instead of the PTF 10ops-like group. Also, some additional objects without enough data to do blue-band fits, SN 2003ae and SN 2007kd, are also classified as a photometric 91bg-like SN Ia according to criterion 1, while spectroscopic classificators indicate it to be a normal SN Ia. These could be like SN 2001bf.

3.6. Other Peculiar SNe Ia

SN 2000cx-like SNe Ia: SN 2000cx-like objects are another class of peculiar, very rare SN Ia objects with only two reported members in the literature, SN 2000cx and SN 2013bh (Silverman et al. 2013b). We obtain very different results with our technique for both. SN 2000cx is quite compatible with a normal SN Ia template, whereas SN 2013bh, having bad fits in both, is slightly more consistent with a 91bg-like SN Ia for the overall and blue-band fits but not for the red-band fits (one of the few objects in quadrant IV in Figure 3). This SN has a blue color, lying far off from SNe Iax, 06bt-like objects, and super-Chandrasekhar SNe Ia in the color–stretch diagram (Figure 6). With such small statistics, it is difficult to conclude much about them and their possible identification, however, if such a blue object, $\mathcal{C} = -0.08$, at mid-stretch, $s_{91\mathrm{bg}} = 1.37$, passing criterion 1 but not 2, is found, it is probably a peculiar SN Ia that does not fit any of the other categories, i.e., it is a SN 2000cx-like object.

Ca-rich transients. Ca-rich transients are an emerging class of objects, possibly thermonuclear in origin (Perets et al. 2010; Kasliwal et al. 2012). Only one of five, SN 2012hn, passes the light curve cuts and has proper SiFTO fits. It is classified as a 91bg-like candidate with the overall fit but there is not enough pre-maximum data in the blue to allow a further identification. If we were to force the fit anyway, we would obtain a better normal blue-band fit. Its extreme red color ($\mathcal{C} = 1.53$) is beyond the extreme cool 91bg-like SNe Ia and the most reddened SNe Ia in the top of Figure 6. Additionally, if one relaxes the light curve coverage cuts, one additional SN, PTF 09dav, a peculiar SN Ia with 91bg-like characteristics (Sullivan et al. 2011), has proper fits and is also classified as a 91bg-like SN Ia with very red color also ($\mathcal{C} = 0.63$). It is then arguably possible to also include Ca-rich transients into the wide variety of peculiar SNe identified with the method presented here. An intriguing transient, SN 2006ha, has similar characteristics: it passes criterion 1 but it does not pass the cuts to check criterion 2, it has a very red color ($\mathcal{C} = 1.06$), and SNID and GELATO tend to find CC or active galactic nucleus matches.

4. DISCUSSION

4.1. Core-collapse Contamination

The versatility of the photometric identification method we present may worry the reader as overly capable of fitting many different objects. What if CC SNe are also incorrectly classified as a peculiar SNe Ia? We investigate this effect in this section by performing the same fits with SiFTO to a large sample of literature CC SNe (Table 3) and an additional sample of SNe II from Anderson et al. (2014). Of the 321 CC SNe in our sample, we obtain proper fits for 64 of them. Of these, only 11 have better overall normal template fits and 53 have better overall 91bg template fits. This is expected as 91bg-like SNe Ia are redder and more easily mistaken with CC SNe, notably SNe Ibc.

To deal with CC contamination, we perform several cuts based on the fit quality in the different filter sets, as well as on the magnitude–color relation shown in Figure 7. In every case, we use a methodology similar to the one presented in Section 2.3 based on the FoM(Ia) and FoM(pec/91bg) to select the best cuts that optimize the number of normal and peculiar SNe Ia correctly tagged and minimize the number of CC SNe falsely tagged. First, for those objects, Ia and CC, having better overall normal template fits, we explore cuts in the fit quality in the range $15 < \chi^2_\nu(\mathrm{Ia}) < 65$ finding a maximum FoM(Ia) at $\chi^2_\nu(\mathrm{Ia}) = 40$ (see the blue line in Figure 10). This cut eliminates four CC SNe and no SN Ia. Similarly, for objects with better overall 91bg template fits, we search for an optimum cut, finding $\chi^2_\nu(91\mathrm{bg}) = 22$ (orange line in Figure 10). This eliminates 17 CC SNe and 3 SNe Ia.

In principle, we could do an equivalent analysis for the fit qualities of blue- and red-band fits searching for cuts that maximize the FoM, but we find that the final FoM does not improve considerably with respect to the overall template fits. On the other hand, we can use the fact that many CC SNe lie outside the typical magnitude relations in Figure 7. However, most effectively, as previously investigated by several authors (e.g., Poznanski et al. 2002; Perets et al. 2011a), the evolution of color and the use of color–color diagrams can be a powerful discriminator between SN groups. Since SiFTO does not enforce any color law for SNe Ia in the fit and allows independent flux factors for each band, we study the evolution of $u' - B$, $B - V$, $V - r'$, and $r' - i'$ colors obtained with the best SiFTO fit. We find that a good discriminator is $B - V$ vs. $u' - B$ at 10 days after the B-band maximum. As shown in the right of Figure 10, CC SNe are redder in $B - V$ and bluer in $u' - B$ than peculiar and 91bg-like SN Ia candidates and more so than normal SNe Ia. Requiring SN Ia candidates to lie underneath the solid line rejects 26 CC SNe with only two peculiar SN Ia discarded. These boundaries are calculated in a similar way as other cuts: we vary the vertical and diagonal lines until we find a maximum FoM(Ia). Our final sample contains 1 CC contaminant that is classified as a normal SN Ia according to the overall fit and four that are tagged as 91bg-like SNe Ia according to the overall fit. All of these are stripped-envelope SNe as expected.

We obtain a final efficiency of $\epsilon(\mathrm{Ia}) \simeq 80\%$ for normal SNe Ia and a purity of $P(\mathrm{Ia}) \simeq 99\%$ from CC SNe and other peculiar SNe Ia resulting in a FoM(Ia) $\simeq$ 80%. This is comparable to other photometric typing techniques as, will be shown in Section 4.4. For 91bg-like SNe Ia/peculiar SNe Ia, we obtain $\epsilon(\mathrm{pec/91bg}) \sim 65\%$ and a purity of $P(\mathrm{pec/91bg}) \sim 85\%$ from CC SNe and normal SNe Ia resulting in a FoM(pec/91bg)$\sim$ 55%. These numbers will be discussed in the next section, where we investigate how strongly the chosen boundaries and cuts depend on the training sample and how they affect the FoMs.

4.2. Bootstrap Analysis

The method we use and the boundaries we define are very sensitive to the sample we use to train the technique. In order to test the importance of this, we perform a bootstrap analysis (Efron 1982) in which different random samples are drawn from the original population to re-do the analysis and calculate the best FoM regions. The bootstrap is done for all SNe Ia and all CC SNe, where objects may be absent in a given iteration and others can also be repeated. For every 1 of the 200 realizations we re-calculate the best cuts presented in Sections 2.3 and 4.1 by finding the maximum FoM box to divide better blue-/red-band normal and 91bg template fits (orange box in Figure 3). We can also find the best χ^2_ν cuts for the overall normal and 91bg template fits to select SNe Ia against CC SNe (lines in Figure 10) for each iteration, as well as the best factor multiplying the magnitude–color median standard deviation to reject CC contamination (dashed lines in Figure 7). The final cuts and errors are calculated taking the mean and standard deviation of all realizations and are summarized in Table 1. The FoMs for each sample with these respective cuts are also presented and the error on the FoM is the FoM calculated at the respective sigma cuts. We emphasize that the quoted FoMs are not the maximum ones, only those based on average cuts. Contamination is taken from CC SNe but also from any other SN Ia sub-sample.

We obtain a robust classification for normal SNe Ia with very low contamination in all realizations of the bootstrap analysis. The peculiar SN Ia identification is more dependent on the sample used for the training and in all cases contains at least seven stripped-envelope CC SNe that lower the purity. Interestingly, these are all classified as 91bg-like objects based on overall, blue-, and red-band fits. So, based on the fit quality in different bands, CC SNe are more easily mistaken with 91bg-like than SNe Iax. However, in the magnitude–color relation, SNe Iax can have extremely low magnitudes for their colors, emulating CC SNe. This means that if no magnitude–color relation for objects with overall 91bg template fits is used, the technique is better at classifying SNe Iax, whereas if one enforces such a cut, then 91bg-like objects will be weighted higher. We note that in the case of a pure SN Ia sample, the blue-/red-band cut of Section 2.3 is sufficient to differentiate between the two: 91bg-like and SNe Iax (and super-Chandra with distinct high stretches).

4.3. Outlook for High-redshift Classification

The technique presented can in principle also be used at higher redshifts. SiFTO has been shown to be a robust light curve fitter across a wide range of redshifts (e.g., Guy et al. 2010; Conley et al. 2011) that works directly with the SED templates in the observer frame, provided an input redshift. For large surveys, this redshift can come from template fitting to multiband photometry from the host galaxy (e.g., Ilbert et al. 2009), as well as from direct SN light curve fits (e.g., Palanque-Delabrouille et al. 2010). Sullivan et al. (2006) and González-Gaitán et al. (2011) used a light curve fitter similar to SiFTO with an additional redshift parameter, which also allows the use of multiple templates such as the 91bg we use here. The particular "blue" and "red" filter sets will need to be adjusted due to redshift effects. For example, while at $z = 0$, a "blue" filter set consists of filters u′g′ and a red filter set of r′i′z′, at $z = 0.5$ these will be u′g′r′ and i′z′, respectively, while at $z = 0.75$ they would move to u′g′r′i′ and z', respectively. Additionally, the cadence and signal-to-noise ratio (S/N) of the data will affect the quality of the light curve fit and could induce mistakes in the classification as well. These effects should be considered when applying this technique to high-z surveys; and they will be investigated in a future work.

4.4. Comparison to Other Classification Techniques

Photometric SN classification is an active area of research. Many early studies, ultimately aimed at cosmology, have focused on normal SN Ia identification either for prioritization in spectral follow-up (Dahlén & Goobar 2002; Sullivan et al. 2006) or posterior identification (e.g., Riess et al. 2004; Barris & Tonry 2006) of real data sets, even in the absence of spectroscopic confirmation (Bazin et al. 2011; Sako et al. 2011b; Perrett et al. 2012; Olmstead et al. 2014) or of simulated samples (Gong et al. 2010; Gjergo et al. 2013). These techniques most often use model template fits to the light curve but also color–color diagrams, as well as host galaxy redshift prior information. The study of multiple SN types, including CC SN classification, is more challenging given the wide diversity of light curve behavior compared to normal SNe Ia. Building on the early efforts by Pskovskii (1978, 1984), more recent methods are color–color evolution (Poznanski et al. 2002; Gal-Yam et al. 2004), color–magnitude evolution (Johnson & Crotts 2006), Bayesian template fitting (Poznanski et al. 2007), Bayesian classification schemes (Kuznetsova & Connolly 2007), Fuzzy Set Theory algorithms

(Rodney & Tonry 2009), boosting and kernel density estimation techniques (Newling et al. 2011), kernel Principal Component Analysis (Ishida & de Souza 2013), a semi-supervised learning (Richards et al. 2012), and neural networks (Karpenka et al. 2013).

A direct comparison to these methods is difficult given the diversity of training samples (although see Kessler et al. 2010a). Nevertheless, we quote some of these studies final efficiencies, purities, and FoM for normal SN Ia classification in Table 4. We caution that, unlike our current study, most of these studies have samples with a wide redshift range, where factors like S/N become important. It is evident that the normal SN Ia classification is quite robust for all different techniques providing clean samples, $P > 90\%$–95% (see also Gjergo et al. 2013; Ishida & de Souza 2013; Karpenka et al. 2013). More challenging is the identification of peculiar groups of SNe Ia, which are more easily mistaken with CC SNe, and the present work is a first step in that direction.

4.5. Photometric "Dromedary" versus "Camel" SN Ia Class

A large range of spectroscopic peculiar SNe Ia are found here to have many similarities in their light curve behavior, resembling those of typical 91bg-like SNe Ia. SNe Iax and super-Chandrasekhar SNe Ia are better fit with a 91bg-like template with SiFTO. This trend is stronger in the redder bands, where post-maximum shoulders and secondary maxima are absent for all of these transients. SN 2006bt-like objects also resemble these, having better red-band 91bg template fits. Grouping them all together, we call them the photometric "dromedary" class, as opposed to classical normal SNe Ia or the photometric "camel" class. For all of these "dromedary" objects, SNe Iax, 06bt-like and super-Chandra, a progressive increase in fit quality (decrease in χ^2_ν) is seen as one moves from short toward longer wavelengths when fitting the light curves with a 91bg template. The opposite occurs when fitting with the normal SN Ia template. If one were to order these groups according to light curve similarities with SiFTO fit quality, one would have 91bg-like → Iax → super-Chandra → 06bt-like → normal SNe Ia.

Furthermore, one can see that the objects of this photometric "dromedary" class (excluding 06bt-like SNe), besides being different from the normal SNe Ia according to two template fits, have different color–stretch (Figure 6) and magnitude–stretch (Figure 7(a)) relations than normal SNe Ia. In particular, they are consistently redder and fainter, i.e., for a particular stretch, different colors and magnitudes are predicted for a normal "camel" SN Ia and a "dromedary" SN. This photometric closeness opens up the question if such a variety of SNe Ia is actually linked to some common physical process, if they arise from similar explosion mechanisms, and even if their progenitors are connected. We examine this further in the following sections.

4.5.1. Cluster Analysis

To investigate the hypothesis of physical commonality of SNe in the "dromedary" class, we perform a cluster analysis (k-means clustering Everitt 1993) in which, given certain SN characteristics, groups of objects more similar to each other than to those of other groups are searched. We provide standardized SiFTO stretch, color, absolute magnitude, and χ^2_ν for overall, blue-, and red-band fits with both normal and 91bg templates for a total of 12 variables for each SN. We present the results of the cluster analysis in Figure 11 requiring $N_{\rm clust} = 2$–5 different cluster groups (from top left to bottom right). Regardless of the number of cluster groups, in each case we observe clear separations between standard SNe Ia and 91bg-like SNe Ia in the top right of each plot. Most of these SNe in the first quadrant are 91bg-like objects, as shown in Figure 3. However, we find that most SNe Iax also make up part of this cluster group (∼five of eight), strengthening the bond between the two peculiar sets. Super-Chandrasekhar and 06bt-like SNe Ia, on the contrary, are always grouped together with normal SNe Ia. This indicates that, even though their light curves have similarities to 91bg-like objects in the redder bands, overall they are more akin to normal SNe Ia, as one would expect. We note that in the first $N_{\rm clust} = 2$ cluster analysis, five quite normal SNe Ia are in the 91bg-like group, which is due to their extreme red colors, e.g., SN 2006X and SN 2003cg, and are put in a different group once we add more cluster groups (or if we do not include color as an input variable). This shows that their colors are of a different nature (interstellar or circumstellar rather than intrinsic) and that the cluster analysis can separate these effects. With $N_{\rm clust} > 3$, the peculiar SN 2005hk, SN 2002es, and some extreme cool 91bg-like are grouped together since they lie off the bulk of the population.

For each cluster analysis, we show the box that best separates the objects in the cluster group similar to 91bg-like from the rest of the groups (cyan solid lines). This is done similarly in Section 2.3 by maximizing the FoM of this cluster group. We find boxes ($\Delta\chi^2_{\nu,\rm red} > 10, 11, 0, 10$ and $\Delta\chi^2_{\nu,\rm blue} > -7, -8, -7, -7$ for each $N_{\rm clust} = 2, 3, 4, 5$ respectively) that compare very well with the box in Figure 3 based on the FoM of known 91bg-objects. This is a strong confirmation of the validity of our technique with an independent and robust approach from data mining. Furthermore, the appearance of this separate region in all cluster analysis strongly supports the hypothesis of clear light curve differences between two SN Ia populations: normal and 91bg-like/Iax SNe. To check for dependence on the sample, we again perform a bootstrap analysis, similar to Section 4.2, finding full consistency with our results. We obtained following 91bg-like boxes based on the mean and standard deviation of all 200 realizations: $\Delta\chi^2_{\nu,\rm red} > 4.8 \pm 8.9, 1.2 \pm 8.0, 0.2 \pm 9.6, 0.6 \pm 9.3$ and $\Delta\chi^2_{\nu,\rm blue} > -10.2 \pm 6.6, -8.6 \pm 7.4, -8.3 \pm 7.9, -7.9 \pm 8.0$ for each $N_{\rm clust} = 2, 3, 4, 5$ respectively.

4.5.2. Environments and Progenitors

From another perspective, the environments of different SNe Ia provide us with important clues about their progenitors. Although classical 91bg-like objects are particularly inclined to occur in elliptical and passive star-forming environments (e.g., Howell 2001; González-Gaitán et al. 2011), PTF 10ops occurred far away from its host (Maguire et al. 2011), SNe Iax seem to prefer late-type galaxies (Lyman et al. 2013; Foley et al. 2013), and super-Chandrasekhar appear in various environments with possible preference for low-mass galaxies (Taubenberger et al. 2011). In Figure 12, we show the morphological type of a large subset of our sample binned in T-types from −5 to 10, from E/S0 galaxies to spiral and irregular galaxies. Performing a Kolmogorov–Smirnov (K-S) test shows that the normal SN Ia distribution (solid blue) is significantly different from the distribution of photometric 91bg-like candidates according to overall, blue-, and red-band fits (dotted orange) with a probability $P(\text{K-S}) \simeq 0.002$. On the other hand, other peculiar SNe Ia according to the overall but not blue or red-band fits, i.e., objects such as PTF 10ops-like, SNe Iax and super-Chandra together (dashed purple) are not statistically different from

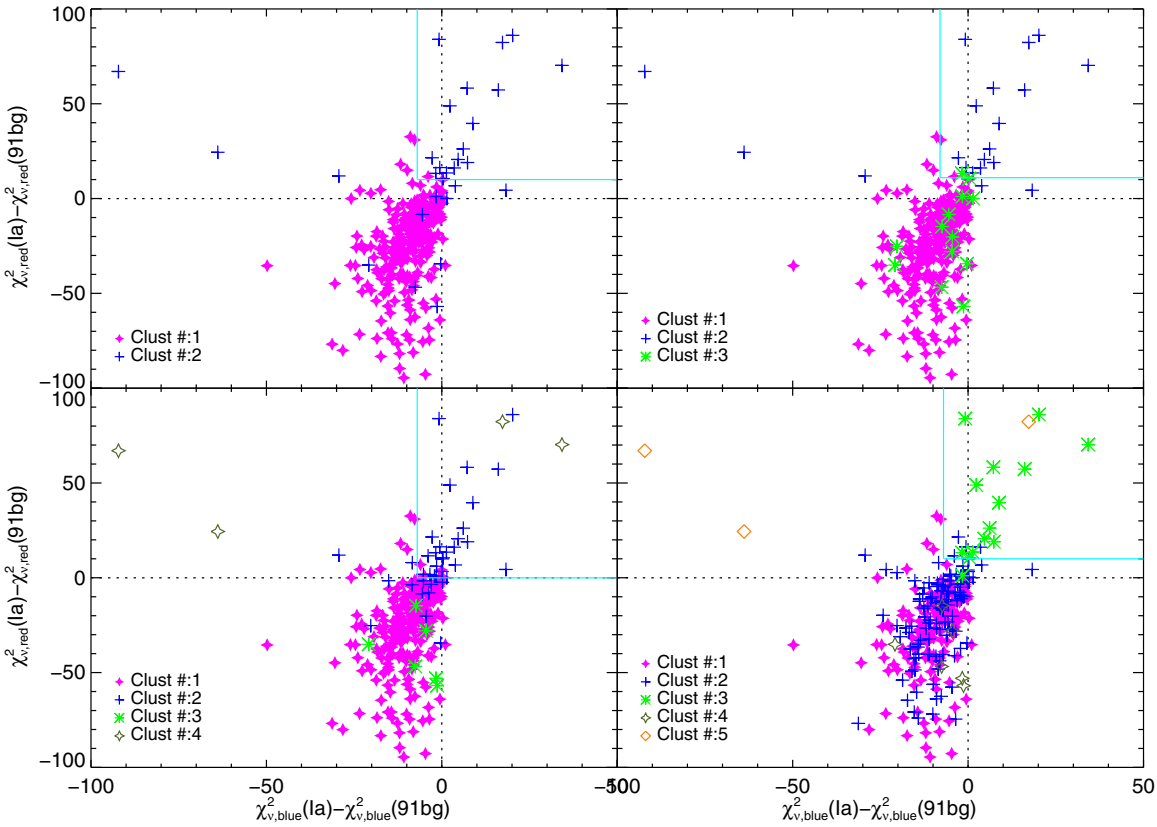

Figure 11. Difference between normal and 91bg template fit qualities in the blue bands $\chi^2_{\nu,\rm blue}(\rm Ia) - \chi^2_{\nu,\rm blue}(\rm 91bg)$ vs. the difference between normal and 91bg template fit qualities in the red bands $\chi^2_{\nu,\rm red}(\rm Ia) - \chi^2_{\nu,\rm red}(\rm 91bg)$ (similar to Figure 3) for different cluster analysis with two (top left) to five (bottom right) cluster groups. The cluster analysis is based on standardized SiFTO stretch, color, absolute magnitude, and overall, blue, and red χ^2_ν for both normal and 91bg templates. Different symbols and colors indicate the groups according to the cluster analysis. Zero χ^2_ν difference dotted lines are shown, and solid cyan lines show the region that optimizes the number of objects of the cluster group in the top right corner of each plot (basically 91bg-like SNe Ia) without objects from other groups.

(A color version of this figure is available in the online journal.)

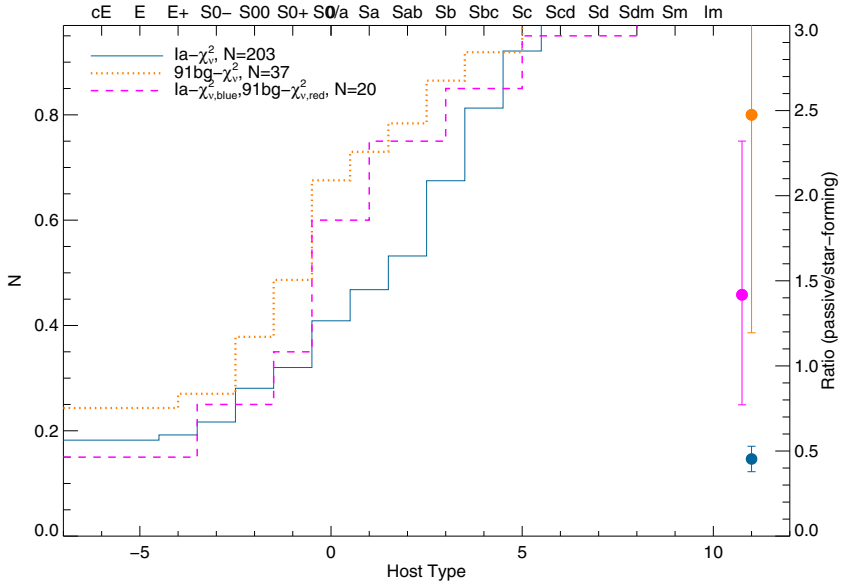

Figure 12. Cumulative distributions of morphological SN host T-type from −5 to 10, where T-types below 0 are passive E/S0 galaxies and types greater than 0 are star-forming galaxies. Different photometric SN Ia groups are shown: normal candidates according to overall, blue-, and red-band fits (solid blue), the 91bg-like candidates according to overall, blue-, and red-band fits (dotted orange), and objects with 91bg-like overall but blue- or red-band normal fits like SNe Iax and super-Chandrasekhar candidates (dashed purple). In the right column, circles show the ratio of passive to star-forming galaxies for the three populations with propagated Poisson errors (Gehrels 1986).

(A color version of this figure is available in the online journal.)

normal SNe Ia (P(K-S) $\simeq 0.12$) or from 91bg-like candidates (P(K-S) $\simeq 0.92$). In the right bin of the figure, we show that the ratio of passive to star forming hosts for the photometric normal SN Ia population (blue circle) is much lower than for the photometric 91bg-like candidates (orange circle), which is a well-known relation. Interestingly, the ratio of the other peculiar SNe Ia (purple circle) lies in between those two samples. A Fisher exact test (Fisher 1922) gives a similar result to the K-S test: the number ratio of photometric normal SNe Ia in passive to star-forming galaxies is statistically different from the ratio of photometric 91bg-like SNe Ia with a probability $P(F) \simeq 0.002$, whereas the ratio for peculiar SNe Ia in passive to star-forming galaxies is not statistically different from the ratio for normal SNe Ia ($P(F) \simeq 0.21$) or from the ratio of 91bg-like SNe Ia (P(F) $\simeq 0.50$). Albeit with low statistics, this may point toward the peculiar SN Ia group being transitional in progenitor characteristics between normal and 91bg-like, or, more likely, it evidences the presence of a mixed group with transitional objects, some 91bg-like and some normal SNe Ia.

From a theoretical standpoint, SNe Iax, SN 1991T, and super-Chandra SNe Ia all have hot, highly ionized photospheres, as has been shown spectroscopically (Foley et al. 2013). In the scenario of Kasen (2006) and Kasen & Woosley (2007), the secondary maximum at long wavelengths can be a direct consequence of the iron group abundance stratification: if the SN has the iron concentrated in the inner region, the recombination of doubly ionized Fe and Co into singly ionized will only occur at later times, redistributing radiation from the blue to the red and creating the secondary maximum. The absence of secondary maxima in red bands for these hot objects can thus be explained with high mixing of ^{56}Ni in the outer layers (see also Scalzo et al. 2012) and argues against a delayed detonation mechanism. In this same framework, the absence of secondary maxima in 91bg-like SNe Ia is explained with quite an opposite argument: these are very cool objects and the recombination therefore sets in much earlier, making the first maximum coincide with the second. So, in one case it is mixing and in the other it is temperature that would explain the post-maximum red-band behavior. Although 91bg-like objects are spectroscopically different to the other peculiar sub-classes, there are some intriguing transitional objects between 91bg-like and Iax with spectroscopic similarities (Ganeshalingam et al. 2012) that may prove a continuous set of explosion mechanisms.

Regarding the progenitor systems, the differences among these peculiar SNe Ia are strengthened. Linking classical 91bg-like and high-stretch PTF 10ops-like SN Ia progenitors, Taubenberger et al. (2013) argue that the nebular spectra of the high-stretch 91bg-like SN 2010lp presents clear evidence for a low density in the core that is only consistent with a violent merger of two CO-WDs (Kromer et al. 2013b). Pakmor et al. (2013), on the other hand, show that 91bg-like explosions can be reproduced via violent mergers of a CO-WD and a He-WD. Super-Chandrasekhar explosions in turn typically invoke slow double-degenerate mergers of massive CO-WDs (e.g., Hachinger et al. 2012). These all invoke variate scenarios of double-degenerate systems. On the contrary, the most favored SN Iax progenitor scenarios are single degenerate in origin: double detonations of a CO-WD and a He-star (Foley et al. 2013; Wang et al. 2013) or pure deflagrations of Chandrasekhar mass WDs (McClelland et al. 2010; Jordan et al. 2012; Kromer et al. 2013a). As for normal SNe Ia, another mechanism, such as the prototypical single-degenerate delayed detonation (e.g., Blondin et al. 2013; Sim et al. 2013) or even double-degenerate mergers with higher WD masses (Pakmor et al. 2013), could explain the differences with the others SNe. Sub-Chandrasekhar explosions have also gained renewed popularity through the double-detonation scenario arising from a shell detonation (Woosley & Weaver 1986; Bildsten et al. 2007; Waldman et al. 2011; Fink et al. 2010), or via violent mergers of two WDs (Pakmor et al. 2012), or even through WD collisions (Benz et al. 1989; Rosswog et al. 2009; Raskin et al. 2009).

Putting this information together, although photometrically the "dromedary" SN Ia class presents interesting common properties among its variate members, such as red color and lack of secondary maxima at longer wavelengths, a cluster analysis suggests that super-Chandrasekhar and 06bt-like are more similar to normal SNe Ia. SNe Iax and 91bg-like SNe are photometrically similar to each other, but they are known to have spectroscopic features that differ, as do their environments. None of the members of the dromedary class can be well explained with a delayed detonation explosion, yet no other clear theoretical link exists among all members of this class. We therefore conclude that although there is probably some common physical mechanism driving the similar behavior in the cooler, redder part of their emission at epochs after maximum, their progenitor and explosion are not necessarily similar in nature.

4.6. Recipe to Photometrically Identify Different SN Ia Sub-groups

In this paper, we have presented a photometric algorithm to identify normal SNe Ia and 91bg-like SNe Ia, the classical fast ones, but also the new class of slowly declining 91bg-like SNe Ia such as PTF 10ops and SN 2010lp. The method also allows us to identify numerous peculiar SNe Ia, particularly SNe Iax, super-Chandrasekhar SNe Ia, and SN 2006bt-like objects. For it to work optimally, we recommend photometry before and after maximum light in several bands, in at least one blue and one red band. At higher distances, where the emission is redshifted, these bands will need to be adjusted. The following is a step-by-step recipe to classify the various events.

1. *SiFTO fits.* Fit each SN with SiFTO using the two templates, normal and 91bg. Also fit each SN with the two templates first using only blue bands and then only red bands.
2. *CC contamination.* Use χ^2_ν cuts to remove CC contamination. For our bootstrapped sample χ^2_ν(Ia) $< 34.0 \pm 6.7$ and χ^2_ν(91bg) $< 21.7 \pm 4.0$ keeps SNe Ia.
3. *Normal SNe Ia.* Objects passing the previous cut and with χ^2_ν(Ia) $- \chi^2_\nu$(91bg) < 0 are normal SN Ia candidates with high confidence. One can reduce the CC contamination of all SNe Ia further with cuts in color–color diagrams. We use $(u - B)_{10} > (0.18 \pm 0.13)$ and $(B - V)_{10} < 0.7(u - B)_{10} + (0.77 \pm 0.23)$. The selected sample may have a very small fraction of objects being of CC.
4. *91bg-like SNe Ia.* Objects that have better overall, blue-band, and red-band 91bg template fits (with a definition of $\chi^2_{\nu,\mathrm{blue,red}}(\mathrm{Ia}) - \chi^2_{\nu,\mathrm{blue,red}}(91\mathrm{bg}) > (-0.8 \pm 2.2), (2.8 \pm 3.1)$) are considered 91bg-like SN Ia candidates. If they have low-stretch, i.e., $s_{91\mathrm{bg}} < 1.1$, then they are classical 91bg-like objects; at higher stretch (and $\mathcal{C} > 0$), they are like PTF 10ops or SN 2010lp.
5. *Super Chandrasekhar SNe Ia.* Those objects with better overall 91bg fits but better normal blue- or red-bands fits, which also have very wide light curves, i.e., $s_{\mathrm{Ia}} > 1.2$ (or $s_{91\mathrm{bg}} > 1.8$), are typical super-Chandrasekhar candidates.

6. *SNe Iax.* SNe Ia with better overall 91bg fits but better normal blue- or red-bands fits, and narrower light curves than in the previous point are probable SNe Iax. There is a possibility that some of these are objects like SN 2002es, of unkown origin or transitional objects, i.e., possibly 91bg-like or SN 2006bt-like, in which case it is not possible to distinguish between those two groups according to our method. Given the numbers, it is more probable (∼83% with the current sample) that such an SN will be a type Iax SN.
7. *SN 2000cx-like SNe Ia.* If the SN Ia has better overall 91bg, but worse red- or blue-band fit, *and* it additionally has a blue color, $\mathcal{C} < 0$, it is most likely not a 91bg-like high-stretch SN Ia or an SN Iax but a peculiar SN 2000cx object, or rather a SN 2013bh-like object.
8. *SN 2006bt-like SNe Ia.* Finally, objects with better overall normal template fit but better red-band 91bg fits and wider light curves ($s_{91bg} > 1.3$) are possibly a group similar to SN 2006bt. These could be a link between normal and super-Chandrasekhar SNe Ia.

5. SUMMARY

We have investigated the light curves of a large sample of low-z SNe Ia with the light curve fitter SiFTO and two spectral template series for normal and SN 1991bg-like SNe Ia. By comparing the fit with the two templates in different filter sets, we are able to photometrically identify typical 91bg-like SNe Ia and also those spectroscopically similar but with wider light curves such as the recent PTF 10ops and SN 2010lp. We confirm the robustness of the technique comparing our photometric classifying technique with different spectroscopic classificators such as SNID. We find that for standard fast-evolving 91bg-like SNe Ia the stretch obtained with a 91bg template fit, s_{91bg}, is better at describing this sub-group than a normal template stretch, s_{Ia}. The existence of two groups is strengthened by a cluster analysis that suggests two different populations based on a set of SN photometric properties. Despite this, we point out the smooth transition between the two and the existence of transitional objects between normal and 91bg-like SNe. Regarding PTF 10ops-like transients, i.e., 91bg-like of wide light curves, we find three to four possible candidates in the literature, confirming the rarity or different environment of such events.

Furthermore, we find a range of transient light curves like SNe Iax, super-Chandrasekhar SNe Ia, and SN 2006bt-like that are more similar to a 91bg-like than a normal template to varying degrees at longer wavelengths. All these "dromedary" objects lack the characteristic prominent secondary maxima or shoulders seen in the red filters of classical SNe Ia and could suggest similar physical processes. Using fit qualities in the different filter sets, we are able to distinguish most of them from typical 91bg-like (which have better 91bg template fits in both the blue and red filter sets) and normal SNe Ia (which have worse 91bg template fits in all filter sets). Of these peculiar objects, SNe Iax generally resemble 91bg-like objects more closely, also in their absolute magnitudes, and some of them can therefore not be differentiated with our technique. The cluster analysis also joins most of SNe Iax with the 91bg-like group, showing that without spectroscopic properties, the light curve differences are not strong enough to form two different groups. Super-Chandra SNe Ia, on the other hand, are clearly distinct in several regards from other peculiar SNe Ia resembling more normal SNe Ia, and it is easy to select them out. We propose an interesting relation between super-Chandra and SN 2006bt-like SNe Ia, with the latter being a less extreme case of the most luminous of SNe Ia, and possibly even also a link between SNe Iax and slowly declining 91bg-like objects.

We have presented a simple yet powerful technique to identify different sub-groups of SNe Ia in a purely photometric manner. With a competitive FoM(Ia) > 80%, we have shown that it robustly classifies normal SNe Ia with very little contamination from CC SNe, but also from other peculiar SNe Ia that are unsuitable for cosmological studies. Alternatively, it also allows us to search for these peculiar SNe Ia to investigate them further: 91bg-like objects, SNe Iax, and even super-Chandrasekhar SNe. Thus, this method is applicable for photometric classification of transients in coming wide field large surveys such as LSST, and to prioritize the study of these interesting peculiar objects, or, on the other hand, to reject them for studies of purely normal SNe Ia.

We thank the anonymous referee for useful comments that improved this work. This paper has made use of a large public data set coming from the long-lasting effort of a variety of surveys and groups, for which we are extremely grateful. The work of C.S.P. has been supported by the National Science Foundation under grants AST 0306969, AST 0607438, and AST 1008343. The CfA Supernova Archive is funded in part by the National Science Foundation through grant AST 0907903. This research has also made use of the NASA/IPAC Extragalactic Database (NED), which is operated by the Jet Propulsion Laboratory, California Institute of Technology, under contract with the National Aeronautics.

S.G., F.B., and L.G. acknowledge support from CONICYT through FONDECYT grants 3130680, 3120227, and 3140566, respectively. Support for S.G., G.P., F.F, C.G, F.B., L.G., M.H., and T.J. is provided by the Ministry of Economy, Development, and Tourism's Millennium Science Initiative through grant IC12009, awarded to The Millennium Institute of Astrophysics, MAS.

REFERENCES

Agnoletto, I., Benetti, S., Cappellaro, E., et al. 2009, ApJ, 691, 1348
Altavilla, G., Fiorentino, G., Marconi, M., et al. 2004, MNRAS, 349, 1344
Anderson, J. P., González-Gaitán, S., Hamuy, M., et al. 2014, ApJ, 786, 67
Anupama, G. C., Sahu, D. K., & Jose, J. 2005, A&A, 429, 667
Barbon, R., Ciatti, F., Iijima, T., & Rosino, L. 1989, A&A, 214, 131
Barbon, R., Ciatti, F., & Rosino, L. 1982, A&A, 116, 35
Barris, B. J., & Tonry, J. L. 2006, ApJ, 637, 427
Bazin, G., Ruhlmann-Kleider, V., Palanque-Delabrouille, N., et al. 2011, A&A, 534, A43
Benetti, S., Cappellaro, E., Mazzali, P. A., et al. 2005, ApJ, 623, 1011
Benetti, S., Cappellaro, E., & Turatto, M. 1991, A&A, 247, 410
Benetti, S., Cappellaro, E., Turatto, M., et al. 1994, A&A, 285, 147
Benetti, S., Meikle, P., Stehle, M., et al. 2004, MNRAS, 348, 261
Benetti, S., Nicholl, M., Cappellaro, E., et al. 2014, MNRAS, 441, 289
Benetti, S., Turatto, M., Balberg, S., et al. 2001, MNRAS, 322, 361
Benz, W., Thielemann, F.-K., & Hills, J. G. 1989, ApJ, 342, 986
Bildsten, L., Shen, K. J., Weinberg, N. N., & Nelemans, G. 2007, ApJL, 662, L95
Biscardi, I., Brocato, E., Arkharov, A., et al. 2012, A&A, 537, A57
Blanton, E. L., Schmidt, B. P., Kirshner, R. P., et al. 1995, AJ, 110, 2868
Blondin, S., Dessart, L., Hillier, D. J., & Khokhlov, A. M. 2013, MNRAS, 429, 2127
Blondin, S., Matheson, T., Kirshner, R. P., et al. 2012, AJ, 143, 126
Blondin, S., & Tonry, J. L. 2007, ApJ, 666, 1024
Bose, S., Kumar, B., Sutaria, F., et al. 2013, MNRAS, 433, 1871
Botticella, M. T., Pastorello, A., Smartt, S. J., et al. 2009, MNRAS, 398, 1041
Bouchet, P., Slezak, E., Le Bertre, T., Moneti, A., & Manfroid, J. 1989, A&AS, 80, 379
Branch, D., Dang, L. C., Hall, N., et al. 2006, PASP, 118, 560
Brown, P. J., Dawson, K. S., Harris, D. W., et al. 2012, ApJ, 749, 18
Brown, P. J., Dessart, L., Holland, S. T., et al. 2007, ApJ, 659, 1488
Brown, P. J., Holland, S. T., Immler, S., et al. 2009, AJ, 137, 4517

Bufano, F., Pian, E., Sollerman, J., et al. 2012, ApJ, 753, 67
Cadonau, R., & Leibundgut, B. 1990, A&AS, 82, 145
Candia, P., Krisciunas, K., Suntzeff, N. B., et al. 2003, PASP, 115, 277
Cao, Y., Kasliwal, M. M., Arcavi, I., et al. 2013, ApJL, 775, L7
Cappellaro, E., Danziger, I. J., della Valle, M., Gouiffes, C., & Turatto, M. 1995, A&A, 293, 723
Chakradhari, N. K., Sahu, D. K., Srivastav, S., & Anupama, G. C. 2014, MNRAS, 443, 1663
Chornock, R., Berger, E., Gezari, S., et al. 2014, ApJ, 780, 44
Chugai, N. N., Fabrika, S. N., Sholukhova, O. N., et al. 2005, AstL, 31, 792
Clocchiatti, A., Suntzeff, N. B., Covarrubias, R., & Candia, P. 2011, AJ, 141, 163
Conley, A., Guy, J., Sullivan, M., et al. 2011, ApJS, 192, 1
Conley, A., Sullivan, M., Hsiao, E. Y., et al. 2008, ApJ, 681, 482
Contreras, C., Hamuy, M., Phillips, M. M., et al. 2010, AJ, 139, 519
Corsi, A., Ofek, E. O., Frail, D. A., et al. 2011, ApJ, 741, 76
Dahlén, T., & Goobar, A. 2002, PASP, 114, 284
D'Andrea, C. B., Sako, M., Dilday, B., et al. 2010, ApJ, 708, 661
Dessart, L., Blondin, S., Brown, P. J., et al. 2008, ApJ, 675, 644
Dessart, L., Blondin, S., Hillier, D. J., & Khokhlov, A. 2014, MNRAS, 441, 532
Di Carlo, E., Massi, F., Valentini, G., et al. 2002, ApJ, 573, 144
Dilday, B., Howell, D. A., Cenko, S. B., et al. 2012, Sci, 337, 942
Drout, M. R., Chornock, R., Soderberg, A. M., et al. 2014, ApJ, 794, 23
Drout, M. R., Soderberg, A. M., Mazzali, P. A., et al. 2013, ApJ, 774, 58
Efron, B. 1982, The Jackknife, the Bootstrap and Other Resampling Plans (CBMS-NSF Monographs, 38; Philadelphia, PA: Society of Industrial and Applied Mathematics)
Elias-Rosa, N., Benetti, S., Cappellaro, E., et al. 2006, MNRAS, 369, 1880
Elias-Rosa, N., Benetti, S., Turatto, M., et al. 2008, MNRAS, 384, 107
Everitt, B. S. 1993, Cluster Analysis (New York: Halsted Press)
Filippenko, A. V., Richmond, M. W., Branch, D., et al. 1992a, AJ, 104, 1543
Filippenko, A. V., Richmond, M. W., Matheson, T., et al. 1992b, ApJL, 384, L15
Fink, M., Röpke, F. K., Hillebrandt, W., et al. 2010, A&A, 514, A53
Fisher, R. A. 1922, J. R. Statis. Soc., 85, 87
Folatelli, G., Contreras, C., Phillips, M. M., et al. 2006, ApJ, 641, 1039
Folatelli, G., Morrell, N., Phillips, M. M., et al. 2013, ApJ, 773, 53
Foley, R. J., Challis, P. J., Chornock, R., et al. 2013, ApJ, 767, 57
Foley, R. J., Challis, P. J., Filippenko, A. V., et al. 2012, ApJ, 744, 38
Foley, R. J., Fox, O. D., McCully, C., et al. 2014, MNRAS, 443, 2887
Foley, R. J., Narayan, G., Challis, P. J., et al. 2010b, ApJ, 708, 1748
Foley, R. J., Papenkova, M. S., Swift, B. J., et al. 2003, PASP, 115, 1220
Foley, R. J., Rest, A., Stritzinger, M., et al. 2010a, AJ, 140, 1321
Ford, C. H., Herbst, W., Richmond, M. W., et al. 1993, AJ, 106, 1101
Fraser, M., Ergon, M., Eldridge, J. J., et al. 2011, MNRAS, 417, 1417
Fraser, M., Inserra, C., Jerkstrand, A., et al. 2013, MNRAS, 433, 1312
Gal-Yam, A., Kasliwal, M. M., Arcavi, I., et al. 2011, ApJ, 736, 159
Gal-Yam, A., Maoz, D., & Sharon, K. 2002, MNRAS, 332, 37
Gal-Yam, A., Mazzali, P., Ofek, E. O., et al. 2009, Natur, 462, 624
Gal-Yam, A., Poznanski, D., Maoz, D., Filippenko, A. V., & Foley, R. J. 2004, PASP, 116, 597
Galama, T. J., Vreeswijk, P. M., van Paradijs, J., et al. 1998, Natur, 395, 670
Gandhi, P., Yamanaka, M., Tanaka, M., et al. 2013, ApJ, 767, 166
Ganeshalingam, M., Li, W., Filippenko, A. V., et al. 2010, ApJS, 190, 418
Ganeshalingam, M., Li, W., Filippenko, A. V., et al. 2012, ApJ, 751, 142
Garnavich, P. M., Bonanos, A. Z., Krisciunas, K., et al. 2004, ApJ, 613, 1120
Gehrels, N. 1986, ApJ, 303, 336
Germany, L. M., Reiss, D. J., Sadler, E. M., Schmidt, B. P., & Stubbs, C. W. 2000, ApJ, 533, 320
Gezari, S., Rest, A., Huber, M. E., et al. 2010, ApJL, 720, L77
Gjergo, E., Duggan, J., Cunningham, J. D., et al. 2013, APh, 42, 52
Goldhaber, G., Groom, D. E., Kim, A., et al. 2001, ApJ, 558, 359
Gong, Y., Cooray, A., & Chen, X. 2010, ApJ, 709, 1420
González-Gaitán, S., Perrett, K., Sullivan, M., et al. 2011, ApJ, 727, 107
Guy, J., Astier, P., Baumont, S., et al. 2007, A&A, 466, 11
Guy, J., Nisini, B., Cabrit, S., Kristensen, L., & Pineau Des Forêts, G. 2010, A&A, 523, A7
Hachinger, S., Mazzali, P. A., Taubenberger, S., et al. 2012, MNRAS, 427, 2057
Hachisu, I., Kato, M., & Nomoto, K. 1996, ApJL, 470, L97
Hamuy, M. 2003, ApJ, 582, 905
Hamuy, M., Phillips, M. M., Maza, J., et al. 1991, AJ, 102, 208
Hamuy, M., Phillips, M. M., Maza, J., et al. 1994, AJ, 108, 2226
Hamuy, M., Phillips, M. M., Suntzeff, N. B., et al. 1996a, AJ, 112, 2408
Hamuy, M., Phillips, M. M., Suntzeff, N. B., et al. 1996b, AJ, 112, 2398
Hamuy, M., Pinto, P. A., Maza, J., et al. 2001, ApJ, 558, 615
Hamuy, M., Suntzeff, N. B., Bravo, J., & Phillips, M. M. 1990, PASP, 102, 888
Harutyunyan, A. H., Pfahler, P., Pastorello, A., et al. 2008, A&A, 488, 383
Hendry, M. A., Smartt, S. J., Crockett, R. M., et al. 2006, MNRAS, 369, 1303
Hicken, M., Challis, P., Jha, S., et al. 2009, ApJ, 700, 331
Hicken, M., Challis, P., Kirshner, R. P., et al. 2012, ApJS, 200, 12
Hicken, M., Garnavich, P. M., Prieto, J. L., et al. 2007, ApJL, 669, L17
Ho, W. C. G., Van Dyk, S. D., Peng, C. Y., et al. 2001, PASP, 113, 1349
Howell, D. A. 2001, ApJL, 554, L193
Howell, D. A., Sullivan, M., Nugent, P. E., et al. 2006, Natur, 443, 308
Hsiao, E. Y., Conley, A., Howell, D. A., et al. 2007, ApJ, 663, 1187
Hunter, D. J., Valenti, S., Kotak, R., et al. 2009, A&A, 508, 371
Iben, I., & Tutukov, A. V. 1984, ApJS, 54, 335
Ilbert, O., Capak, P., Salvato, M., et al. 2009, ApJ, 690, 1236
Inserra, C., Pastorello, A., Turatto, M., et al. 2013a, A&A, 555, A142
Inserra, C., Smartt, S. J., Jerkstrand, A., et al. 2013b, ApJ, 770, 128
Inserra, C., Turatto, M., Pastorello, A., et al. 2012, MNRAS, 422, 1122
Ishida, E. E. O., & de Souza, R. S. 2013, MNRAS, 430, 509
Ivezic, Z., Strauss, M. A., Tyson, J. A., et al. 2011, BAAS, 43, 252.01
Jha, S., Kirshner, R. P., Challis, P., et al. 2006, AJ, 131, 527
Jha, S., Riess, A. G., & Kirshner, R. P. 2007, ApJ, 659, 122
Johnson, B. D., & Crotts, A. P. S. 2006, AJ, 132, 756
Jordan, G. C., IV, Perets, H. B., Fisher, R. T., & van Rossum, D. R. 2012, ApJL, 761, L23
Kamiya, Y., Tanaka, M., Nomoto, K., et al. 2012, ApJ, 756, 191
Kankare, E., Ergon, M., Bufano, F., et al. 2012, MNRAS, 424, 855
Kankare, E., Mattila, S., Ryder, S., et al. 2014, MNRAS, 440, 1052
Karpenka, N. V., Feroz, F., & Hobson, M. P. 2013, MNRAS, 429, 1278
Kasen, D. 2006, ApJ, 649, 939
Kasen, D., & Woosley, S. E. 2007, ApJ, 656, 661
Kashi, A., & Soker, N. 2011, MNRAS, 417, 1466
Kasliwal, M. M., Kulkarni, S. R., Gal-Yam, A., et al. 2010, ApJL, 723, L98
Kasliwal, M. M., Kulkarni, S. R., Gal-Yam, A., et al. 2012, ApJ, 755, 161
Kasliwal, M. M., Ofek, E. O., Gal-Yam, A., et al. 2008, ApJL, 683, L29
Kawabata, K. S., Tanaka, M., Maeda, K., et al. 2009, ApJ, 697, 747
Kessler, R., Bassett, B., Belov, P., et al. 2010a, PASP, 122, 1415
Kessler, R., Cinabro, D., Bassett, B., et al. 2010b, ApJ, 717, 40
Khan, R., Prieto, J. L., Pojmanski, G., et al. 2011, ApJ, 726, 106
Kimeridze, G. N., & Tsvetkov, D. Y. 1991, AZh, 68, 341
Kleiser, I. K. W., Poznanski, D., Kasen, D., et al. 2011, MNRAS, 415, 372
Kowalski, M., Rubin, D., Aldering, G., et al. 2008, ApJ, 686, 749
Krisciunas, K., Hamuy, M., Suntzeff, N. B., et al. 2009, AJ, 137, 34
Krisciunas, K., Hastings, N. C., Loomis, K., et al. 2000, ApJ, 539, 658
Krisciunas, K., Phillips, M. M., Stubbs, C., et al. 2001, AJ, 122, 1616
Krisciunas, K., Phillips, M. M., Suntzeff, N. B., et al. 2004a, AJ, 127, 1664
Krisciunas, K., Prieto, J. L., Garnavich, P. M., et al. 2006, AJ, 131, 1639
Krisciunas, K., Suntzeff, N. B., Candia, P., et al. 2003, AJ, 125, 166
Krisciunas, K., Suntzeff, N. B., Phillips, M. M., et al. 2004b, AJ, 128, 3034
Kromer, M., Fink, M., Stanishev, V., et al. 2013a, MNRAS, 429, 2287
Kromer, M., Pakmor, R., Taubenberger, S., et al. 2013b, ApJL, 778, L18
Kromer, M., Sim, S. A., Fink, M., et al. 2010, ApJ, 719, 1067
Kumar, B., Pandey, S. B., Sahu, D. K., et al. 2013, MNRAS, 431, 308
Kuznetsova, N. V., & Connolly, B. M. 2007, ApJ, 659, 530
Lair, J. C., Leising, M. D., Milne, P. A., & Williams, G. G. 2006, AJ, 132, 2024
Leibundgut, B., Kirshner, R. P., Phillips, M. M., et al. 1993, AJ, 105, 301
Leonard, D. C., Filippenko, A. V., Gates, E. L., et al. 2002a, PASP, 114, 35
Leonard, D. C., Filippenko, A. V., Li, W., et al. 2002b, AJ, 124, 2490
Leonard, D. C., Li, W., Filippenko, A. V., Foley, R. J., & Chornock, R. 2005, ApJ, 632, 450
Li, W., Filippenko, A. V., Chornock, R., et al. 2003, PASP, 115, 453
Li, W., Filippenko, A. V., Gates, E., et al. 2001, PASP, 113, 1178
Li, W., Leaman, J., Chornock, R., et al. 2011, MNRAS, 412, 1441
Lira, P., Suntzeff, N. B., Phillips, M. M., et al. 1998, AJ, 115, 234
Lorén-Aguilar, P., Isern, J., & García-Berro, E. 2009, A&A, 500, 1193
Lunnan, R., Chornock, R., Berger, E., et al. 2013, ApJ, 771, 97
Lyman, J. D., James, P. A., Perets, H. B., et al. 2013, MNRAS, 434, 527
Maeda, K., Kawabata, K., Li, W., et al. 2009, ApJ, 690, 1745
Maguire, K., Sullivan, M., Thomas, R. C., et al. 2011, MNRAS, 418, 747
Malesani, D., Tagliaferri, G., Chincarini, G., et al. 2004, ApJL, 609, L5
Maoz, D., Mannucci, F., & Nelemans, G. 2014, ARA&A, 52, 107
Marion, G. H., Sand, D. J., Hsiao, E. Y., et al. 2014b, arXiv:1405.3970
Marion, G. H., Vinko, J., Kirshner, R. P., et al. 2014a, ApJ, 781, 69
McCully, C., Jha, S. W., Foley, R. J., et al. 2014, ApJ, 786, 134
Mauerhan, J. C., Smith, N., Silverman, J. M., et al. 2013, MNRAS, 431, 2599
Maza, J., Hamuy, M., Phillips, M. M., Suntzeff, N. B., & Aviles, R. 1994, ApJL, 424, L107
Mazzali, P. A., Röpke, F. K., Benetti, S., & Hillebrandt, W. 2007, Sci, 315, 825
McClelland, C. M., Garnavich, P. M., Galbany, L., et al. 2010, ApJ, 720, 704
McKenzie, E. H., & Schaefer, B. E. 1999, PASP, 111, 964
Meikle, W. P. S., Cumming, R. J., Geballe, T. R., et al. 1996, MNRAS, 281, 263

Miller, A. A., Silverman, J. M., Butler, N. R., et al. 2010, MNRAS, 404, 305
Misra, K., Pooley, D., Chandra, P., et al. 2007, MNRAS, 381, 280
Modjaz, M., Li, W., Butler, N., et al. 2009, ApJ, 702, 226
Munari, U., Henden, A., Belligoli, R., et al. 2013, NewA, 20, 30
Newling, J., Varughese, M., Bassett, B., et al. 2011, MNRAS, 414, 1987
Nicholl, M., Smartt, S. J., Jerkstrand, A., et al. 2013, Natur, 502, 346
Nomoto, K. 1982, ApJ, 257, 780
Nomoto, K., Thielemann, F.-K., & Yokoi, K. 1984, ApJ, 286, 644
Nugent, P., Kim, A., & Perlmutter, S. 2002, PASP, 114, 803
Ofek, E. O., Sullivan, M., Cenko, S. B., et al. 2013, Natur, 494, 65
Olmstead, M. D., Brown, P. J., Sako, M., et al. 2014, AJ, 147, 75
Pakmor, R., Kromer, M., Taubenberger, S., & Springel, V. 2013, ApJL, 770, L8
Pakmor, R., Kromer, M., Taubenberger, S., et al. 2012, ApJL, 747, L10
Palanque-Delabrouille, N., et al. 2010, A&A, 514, A63
Pan, Y. C., Sullivan, M., Maguire, K., et al. 2014, MNRAS, 438, 1391
Pastorello, A., Quimby, R. M., Smartt, S. J., et al. 2008, MNRAS, 389, 131
Pastorello, A., Smartt, S. J., Botticella, M. T., et al. 2010, ApJL, 724, L16
Pastorello, A., Taubenberger, S., Elias-Rosa, N., et al. 2007, MNRAS, 376, 1301
Pastorello, A., Valenti, S., Zampieri, L., et al. 2009, MNRAS, 394, 2266
Pastorello, A., Zampieri, L., Turatto, M., et al. 2004, MNRAS, 347, 74
Patat, F., Benetti, S., Cappellaro, E., et al. 1996, MNRAS, 278, 111
Pennypacker, C. R., Burns, M. S., Crawford, F. S., et al. 1989, AJ, 97, 186
Perets, H. B., Badenes, C., Arcavi, I., Simon, J. D., & Gal-yam, A. 2011a, ApJ, 730, 89
Perets, H. B., Gal-yam, A., Crockett, R. M., et al. 2011b, ApJL, 728, L36
Perets, H. B., Gal-Yam, A., Mazzali, P. A., et al. 2010, Natur, 465, 322
Perlmutter, S., Aldering, G., Goldhaber, G., et al. 1999, ApJ, 517, 565
Perlmutter, S., Gabi, S., Goldhaber, G., et al. 1997, ApJ, 483, 565
Perrett, K., Sullivan, M., Conley, A., et al. 2012, AJ, 144, 59
Phillips, M. M. 1993, ApJL, 413, L105
Phillips, M. M. 2012, PASA, 29, 434
Phillips, M. M., Krisciunas, K., Suntzeff, N. B., et al. 2006, AJ, 131, 2615
Phillips, M. M., Li, W., Frieman, J. A., et al. 2007, PASP, 119, 360
Phillips, M. M., Phillips, A. C., Heathcote, S. R., et al. 1987, PASP, 99, 592
Phillips, M. M., Wells, L. A., Suntzeff, N. B., et al. 1992, AJ, 103, 1632
Pian, E., Mazzali, P. A., Masetti, N., et al. 2006, Natur, 442, 1011
Pignata, G., Benetti, S., Mazzali, P. A., et al. 2008, MNRAS, 388, 971
Pignata, G., Patat, F., Benetti, S., et al. 2004, MNRAS, 355, 178
Pignata, G., Stritzinger, M., Soderberg, A., et al. 2011, ApJ, 728, 14
Poznanski, D., Chornock, R., Nugent, P. E., et al. 2010, Sci, 327, 58
Poznanski, D., Gal-Yam, A., Maoz, D., et al. 2002, PASP, 114, 833
Poznanski, D., Maoz, D., & Gal-Yam, A. 2007, AJ, 134, 1285
Pozzo, M., Meikle, W. P. S., Rayner, J. T., et al. 2006, MNRAS, 368, 1169
Prieto, J. L., Lee, J. C., Drake, A. J., et al. 2012, ApJ, 745, 70
Prieto, J. L., Garnavich, P. M., Phillips, M. M., et al. 2007, arXiv:0706.4088
Pritchard, T. A., Roming, P. W. A., Brown, P. J., Bayless, A. J., & Frey, L. H. 2014, ApJ, 787, 157
Pskovskii, I. P. 1978, SvA, 22, 201
Pskovskii, Y. P. 1984, SvA, 28, 658
Raskin, C., Timmes, F. X., Scannapieco, E., Diehl, S., & Fryer, C. 2009, MNRAS, 399, L156
Richards, J. W., Homrighausen, D., Freeman, P. E., Schafer, C. M., & Poznanski, D. 2012, MNRAS, 419, 1121
Richmond, M. W., & Smith, H. A. 2012, JAAVSO, 40, 872
Richmond, M. W., Treffers, R. R., Filippenko, A. V., et al. 1995, AJ, 109, 2121
Riess, A. G., Filippenko, A. V., Challis, P., et al. 1998, AJ, 116, 1009
Riess, A. G., Kirshner, R. P., Schmidt, B. P., et al. 1999, AJ, 117, 707
Riess, A. G., Li, W., Stetson, P. B., et al. 2005, ApJ, 627, 579
Riess, A. G., Press, W. H., & Kirshner, R. P. 1996, ApJ, 473, 88
Riess, A. G., Strolger, L.-G., Tonry, J., et al. 2004, ApJ, 607, 665
Rodney, S. A., & Tonry, J. L. 2009, ApJ, 707, 1064
Rosswog, S., Kasen, D., Guillochon, J., & Ramirez-Ruiz, E. 2009, ApJL, 705, L128
Roy, R., Kumar, B., Benetti, S., et al. 2011a, ApJ, 736, 76
Roy, R., Kumar, B., Maund, J. R., et al. 2013, MNRAS, 434, 2032
Roy, R., Kumar, B., Moskvitin, A. S., et al. 2011b, MNRAS, 414, 167
Sadakane, K., Yokoo, T., Arimoto, J.-I., et al. 1996, PASJ, 48, 51
Sahu, D. K., Anupama, G. C., & Chakradhari, N. K. 2013, MNRAS, 433, 2
Sahu, D. K., Gurugubelli, U. K., Anupama, G. C., & Nomoto, K. 2011, MNRAS, 413, 2583
Sako, M., Bassett, B., Becker, A. C., et al. 2014, arXiv:1401.3317
Sako, M., Bassett, B., Connolly, B., et al. 2011b, ApJ, 738, 162
Sako, M. Dark Energy Survey DES Supernova Working Group, & DES Collaboration. 2011a, BAAS, 43, 205.07
Salvo, M. E., Cappellaro, E., Mazzali, P. A., et al. 2001, MNRAS, 321, 254
Scalzo, R. A., Aldering, G., Antilogus, P., et al. 2010, ApJ, 713, 1073
Scalzo, R., Aldering, G., Antilogus, P., et al. 2012, ApJ, 757, 12
Scalzo, R. A., Childress, M., Tucker, B., et al. 2014, MNRAS, 445, 30
Schlafly, E. F., & Finkbeiner, D. P. 2011, ApJ, 737, 103
Schmidt, B. P., Kirshner, R. P., Eastman, R. G., et al. 1994, ApJ, 432, 42
Schmidt, B. P., Kirshner, R. P., Schild, R., et al. 1993, AJ, 105, 2236
Shen, K. J., Bildsten, L., Kasen, D., & Quataert, E. 2012, ApJ, 748, 35
Silverman, J. M., Foley, R. J., Filippenko, A. V., et al. 2012, MNRAS, 425, 1789
Silverman, J. M., Nugent, P. E., Gal-Yam, A., et al. 2013a, ApJS, 207, 3
Silverman, J. M., Vinko, J., Kasliwal, M. M., et al. 2013b, MNRAS, 436, 1225
Sim, S. A., Röpke, F. K., Hillebrandt, W., et al. 2010, ApJL, 714, L52
Sim, S. A., Seitenzahl, I. R., Kromer, M., et al. 2013, MNRAS, 436, 333
Smartt, S. J., Eldridge, J. J., Crockett, R. M., & Maund, J. R. 2009, MNRAS, 395, 1409
Smith, N., Ganeshalingam, M., Chornock, R., et al. 2009, ApJL, 697, L49
Smith, N., Mauerhan, J. C., Silverman, J. M., et al. 2012, MNRAS, 426, 1905
Sollerman, J., Cumming, R. J., & Lundqvist, P. 1998, ApJ, 493, 933
Stoll, R., Prieto, J. L., Stanek, K. Z., et al. 2011, ApJ, 730, 34
Stritzinger, M., Hamuy, M., Suntzeff, N. B., et al. 2002, AJ, 124, 2100
Stritzinger, M., Mazzali, P., Phillips, M. M., et al. 2009, ApJ, 696, 713
Stritzinger, M., Taddia, F., Fransson, C., et al. 2012, ApJ, 756, 173
Stritzinger, M. D., Hsiao, E., Valenti, S., et al. 2014, A&A, 561, A146
Stritzinger, M. D., Phillips, M. M., Boldt, L. N., et al. 2011, AJ, 142, 156
Strolger, L., Smith, R. C., Suntzeff, N. B., et al. 2002, AJ, 124, 2905
Sullivan, M., Howell, D. A., Perrett, K., et al. 2006, AJ, 131, 960
Sullivan, M., Kasliwal, M. M., Nugent, P. E., et al. 2011, ApJ, 732, 118
Suntzeff, N. B., Phillips, M. M., Covarrubias, R., et al. 1999, AJ, 117, 1175
Suzuki, N., Rubin, D., Lidman, C., et al. 2012, ApJ, 746, 85
Taddia, F., Stritzinger, M. D., Phillips, M. M., et al. 2012a, A&A, 545, L7
Taddia, F., Stritzinger, M. D., Sollerman, J., et al. 2012b, A&A, 537, A140
Taddia, F., Stritzinger, M. D., Sollerman, J., et al. 2013, A&A, 555, A10
Takats, K., Pumo, M. L., Elias-Rosa, N., et al. 2014, MNRAS, 438, 368
Tanaka, M., Yamanaka, M., Maeda, K., et al. 2009, ApJ, 700, 1680
Taubenberger, S., Benetti, S., Childress, M., et al. 2011, MNRAS, 412, 2735
Taubenberger, S., Hachinger, S., Pignata, G., et al. 2008, MNRAS, 385, 75
Taubenberger, S., Kromer, M., Pakmor, R., et al. 2013, ApJL, 775, L43
Taubenberger, S., Pastorello, A., Mazzali, P. A., et al. 2006, MNRAS, 371, 1459
Tomasella, L., Cappellaro, E., Fraser, M., et al. 2013, MNRAS, 434, 1636
Tripp, R. 1998, A&A, 331, 815
Trundle, C., Pastorello, A., Benetti, S., et al. 2009, A&A, 504, 945
Tsvetkov, D. I., Volkov, I. M., Bartunov, O. S., Ikonnikova, N. P., & Kimeridze, G. N. 1990, A&A, 236, 133
Tsvetkov, D. Y. 2006a, PZ, 26, 3
Tsvetkov, D. Y. 2006b, PZ, 26, 4
Tsvetkov, D. Y. 2008, PZ, 28, 3
Tsvetkov, D. Y., Balanutsa, P., Gorbovskoy, E., et al. 2010, PZ, 30, 3
Tsvetkov, D. Y., Balanutsa, P. V., Lipunov, V. M., et al. 2011, AstL, 37, 775
Tsvetkov, D. Y., & Elenin, L. 2010, PZ, 30, 2
Tsvetkov, D. Y., Goranskij, V., & Pavlyuk, N. 2008, PZ, 28, 8
Tsvetkov, D. Y., Metlov, V. G., Shugarov, S. Y., Tarasova, T. N., & Pavlyuk, N. N. 2014, arXiv:1403.7405
Tsvetkov, D. Y., Muminov, M., Burkhanov, O., & Kahharov, B. 2007, PZ, 27, 5
Tsvetkov, D. Y., Volnova, A. A., Shulga, A. P., et al. 2006, A&A, 460, 769
Turatto, M., Cappellaro, E., Benetti, S., & Danziger, I. J. 1993, MNRAS, 265, 471
Valenti, S., Benetti, S., Cappellaro, E., et al. 2008, MNRAS, 383, 1485
Valenti, S., Fraser, M., Benetti, S., et al. 2011, MNRAS, 416, 3138
Valenti, S., Pastorello, A., Cappellaro, E., et al. 2009, Natur, 459, 674
Valenti, S., Sand, D., Pastorello, A., et al. 2014b, MNRAS, 438, L101
Valenti, S., Taubenberger, S., Pastorello, A., et al. 2012, ApJL, 749, L28
Valenti, S., Yuan, F., Taubenberger, S., et al. 2014a, MNRAS, 437, 1519
Valentini, G., Di Carlo, E., Massi, F., et al. 2003, ApJ, 595, 779
Waldman, R., Sauer, D., Livne, E., et al. 2011, ApJ, 738, 21
Wang, B., Justham, S., & Han, Z. 2013, A&A, 559, A94
Wang, X., Filippenko, A. V., Ganeshalingam, M., et al. 2009a, ApJL, 699, L139
Wang, X., Li, W., Filippenko, A. V., et al. 2009b, ApJ, 697, 380
Wells, L. A., Phillips, M. M., Suntzeff, B., et al. 1994, AJ, 108, 2233
Wheeler, J. C. 2012, ApJ, 758, 123
White, C. J., Kasliwal, M. M., Nugent, P. E., et al. 2014, arXiv:1405.7409
Woosley, S. E., & Weaver, T. A. 1986, ARA&A, 24, 205
Yoshii, Y., Tomita, H., Kobayashi, Y., et al. 2003, ApJ, 592, 467
Young, D. R., Smartt, S. J., Valenti, S., et al. 2010, A&A, 512, A70
Younger, P. F., & van den Bergh, S. 1985, A&AS, 61, 365
Zhang, T., Wang, X., Li, W., et al. 2010, PASP, 122, 1
Zhang, T., Wang, X., Wu, C., et al. 2012, AJ, 144, 131